공학석사학위논문

Blade Configuration Design for Lift-Offset Compound Helicopter on the stage of Conceptual Design

개념 설계 단계에서의 Lift-Offset 복합형 회전익기 블레이드 형상 설계 연구

2023년 2월

서울대학교 대학원

항공우주공학과

국 효 진

Blade Configuration Design for Lift-Offset Compound Helicopter on the stage of Conceptual Design

개념 설계 단계에서의 Lift-Offset 복합형 회전익기 블레이드 형상 설계 연구

지도교수 이 관 중

이 논문을 공학석사 학위논문으로 제출함

2023년 2월

서울대학교 대학원

항공우주공학과

국 효 진

국효진의 공학석사 학위논문을 인준함

2023년 2월

위 원 장 김규홍 (인)

부위원장 이관중 (인)

위 원 권기범 (인)

Abstract

Low efficiency in high−speed forward flight due to dynamic stall on a retreating side is a disadvantage of conventional single−rotor helicopters that is difficult to improve. Lift−offset is a technique to overcome this disadvantage by increasing the efficiency in high−speed forward flight by creating the maximum lift that can be generated on an advancing side even if lift loss occurs on a retreating side. In addition, the development of a stiff hingeless rotor makes it possible to drive rotors even when a non−small roll moment was created due to an imbalanced lift on the advancing and retreating sides.

However, a lift−offset coaxial rotor was analyzed using high−fidelity tools represented by CAMRAD II and computational fluid analysis because of complex flow phenomena such as the interference effect between the upper and lower rotors. This paper developed a lift−offset coaxial rotor analysis module that modified the blade−element theory and applied it to RISPECT+, a vertical take−off and landing aircraft sizing tool. Through this, a process of designing a lift−offset compound helicopter with lower time and cost is proposed.

Initial sizing of a compound helicopter with a single pusher propeller and a lift-offset coaxial rotor was performed using the proposed conceptual design process. Furthermore, the airfoil design of rotor blades was additionally conducted in the conceptual design stage, and the effect of the aerodynamic performance of rotors on the conceptual design results was quantitatively investigated by considering airfoil design at the conceptual design stage. The airfoil design was carried out using the Improved Geometric Parameter (IGP) method after dividing the rotor blade into three sections and analyzing flow analysis conditions. After performing the optimization design process using the NSGA-II algorithm and XFOIL, an improved conceptual design result was derived by applying designed airfoils. As a result, it is concluded that improved design results for the lift-offset coaxial rotor, which greatly affects the total weight and required power of the lift-offset compound helicopter, can be obtained by proceeding with the airfoil design using the improved rotor analysis module in the conceptual design stage.

Keyword : Lift-Offset Coaxial Rotor, Conceptual Design, Rotor Blade Configuration Design

Student Number : 2021-26710

Table of Contents

List of Figures

List of Tables

Chapter 1. Introduction

Although helicopters are capable of vertical take-off and landing, different aerodynamic characteristics appear on the advancing and retreating sides due to the imbalance of lift generation on the rotor plane during forward flight. In forward flight, in the case of a conventional single-rotor helicopter, there is a limitation that it cannot generate maximum lift on the advancing side due to low dynamic pressure and stall on the retreating side[1]. This phenomenon occurs because the roll moment generated on the advancing and retreating sides must be balanced. Because the amount of roll moment that can be handled by an articulated hub is not large. Inevitably, the rotor cannot produce the maximum thrust in terms of efficiency, and the efficiency further decreases as the advance ratio increases[2]. Therefore, the disadvantages of conventional helicopters in the form of a single rotor that cannot achieve high speed during forward flight and require more power have been continuously pointed out. Demand to diversify the use of vertical take-off and landing aircraft by overcoming the limitations of cruising speed and range of existing single-rotor helicopters has continued to exist. With the development of a stiff hingeless rotor that can handle a roll moment of sufficient magnitude, a movement to apply lift-offset maneuvers to actual helicopters has emerged to meet these demands.

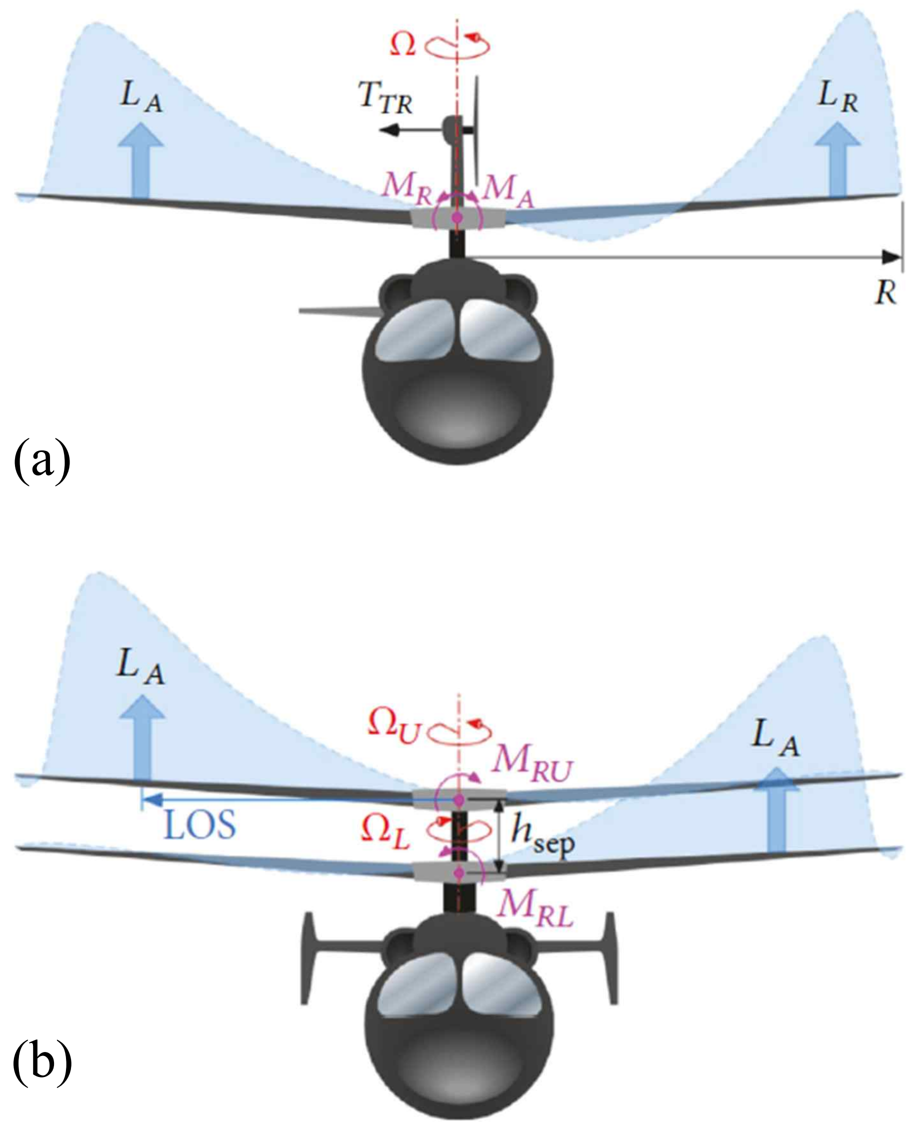

Figure 1. Lift and roll moment characteristics [3]
(a) Conventional Single rotor and (b) Rigid Coaxial rotor with Lift-offset

Lift-offset is a concept that generates the maximum possible lift on the advancing side even if there is a loss of lift on the retreating side. With the development of a stiff hingeless rotor, the rotor could be driven even when a large roll moment was created due to an unbalanced lift. The ABC(Advancing Blade Concept) rotor was developed in the form of a coaxial rotor in which these stiff hingeless rotors are placed at the upper and lower to balance the roll moment in the entire rotor system by generating roll moments in opposite directions on the upper and lower rotors[4]. During lift-offset maneuver, since the center of lift on the rotor disc moves toward the advancing side, stall on the retreating side can be prevented, and maximum lift-to-drag ratio can be achieved on the advancing side[5].

In this regard, Sikorsky introduced significant research results by studying the aerodynamic optimum design of rotor blades and hubs and a new concept of hub control mechanisms. First, the rotor technology of the ABC (Advancing Blade Concept), which added a lift-offset maneuver to a stiff hingeless rotor in the 1970s, was introduced through a test flight of the XH-59A[4]. In addition, based on the technology developed through the XH-59A in the FVL (Future Vertical Lift) project[6] in the US, technology for a high-speed lift-offset compound helicopter was developed through the 5,500lb class X2 technology™ demonstrator[7] in 2008. In 2015, the test flight of the 11,000lb class S-97 Raider[8] equipped with a lift-offset coaxial rotor was also successful. Since then, the 30,000lb class SB>1 Defiant was developed as a medium-sized FVL technology demonstrator with Boeing, and the first flight was successful in 2019, and the SB>1 DefiantX is under development in 2021. The US Army is also actively supporting the development of Sikorsky-Boeing's SB>1 Defiant X coaxial compound helicopter through its FLRAA (Future Long Range Assault Aircraft) development plan.

Figure 2. (a) XH-59A (b) X2 Technology™ Demonstrator (c) S-97 Raider (d) SB>1 Defiant

In order to maximize performance in high-speed forward flight, these aircraft are being developed in the form of a compound helicopter that uses a main rotor system with lift-offset maneuver and an auxiliary thrust device such as a pusher propeller and a jet engine. During high-speed forward flight, a slowdown condition that reduces the rotational speed of the rotor is applied to prevent stall and shock waves generated from the rotor due to high flow speed The forward speed may not be reduced when used in conjunction with auxiliary thrust devices. However, in this process, the power required for forward flight increases due to the increase in drag of the rotor blades. Accordingly, a vicious cycle of increasing engine weight, helicopter weight, and fuel consumption is generated. Therefore, in order to design a compound helicopter, it is essential to consider its blades' configuration, the aerodynamics and structural loads, and the interaction between its upper and lower rotors.

In the studies conducted so far, analysis of the coaxial lift-offset rotor was conducted using a high-fidelity tool such as CAMRAD II[9] and CFD (Computational Fluid Dynamics) in order to improve the prediction accuracy of the vibration and aerodynamic performance of the lift-offset coaxial rotor. Roland et al., 2019[10] compared CAMRAD II and wind tunnel test results to secure reliability in predicting the vibration and aerodynamic performance of a coaxial lift-offset rotor. In the thesis of Kwon, 2021[11], CAMRAD II was used to predict the required power of the X2 technology demonstrator, and the results were compared with the flight test results. In addition, Yeo, 2014[12] performed modeling of the XH-59A using NDARC and CAMRAD II and quantitatively presented the effect of lift-offset maneuver on the aerodynamic performance of the rotor and the total required power of the compound helicopter. According to the study, the greater the roll moment applied to the upper and lower rotors, the higher the efficiency in forward flight. However, since the flap bending moment of the blade is greatly affected by the hub roll moment, the lift-offset maneuver must be properly controlled.

However, in the conceptual design stage of a compound helicopter, such a high-fidelity tool has the disadvantage of too many parameters to consider and a high computational cost. Therefore, in this study, a coaxial lift-offset rotor analysis module that can be used in the concept design stage is developed by modifying the blade element theory used for a single rotor. In addition, the developed analysis module is verified by comparing it with the flight test results of the XH-59A. Moreover, a conceptual design process for a lift-offset compound helicopter considering the drag of the auxiliary thrust device and fuselage, and the aerodynamic performance of the coaxial lift-offset rotor is proposed. Based on the proposed conceptual design process, the results of the conceptual design of a lift-offset compound helicopter are presented using the military mission and design requirements proposed by Johnson, 2012[13].

Additionally, in this study, the configuration design of the airfoil to be applied to the rotor blade is carried out using the analysis result of the coaxial lift-offset rotor derived from the conceptual design process. Unlike the conventional single rotor, the coaxial lift-offset rotor experiences complex flow phenomena such as interference between the upper and lower rotors. Considering this, a new airfoil design process that can be implemented in the conceptual design stage is proposed. Through this, the optimized coaxial lift-offset rotor blade configuration is designed in a short time, and the result is applied to the concept design of the compound helicopter.

Chapter 2. Conceptual design process

2.1. Conceptual design tool for a vertical take−off and landing aircraft

The conceptual design process for a lift−offset compound helicopter is based on RISPECT+ (Rotorcraft Initial Sizing and Performance Estimation Code and Toolkit+)[14], an integrated analysis program for a vertical take−off and landing aircraft. RISPECT+ aims to derive the weight information for the requested mission by receiving design variables such as the number of blades, radius, and chord length of a rotor. In addition, the vehicle sizing optimized for the overall mission profile is performed by calculating the required power and fuel consumption through trim and performance analysis, engine sizing, and weight estimation according to the mission of the aircraft. Figure 3 shows the flowchart of RISPECT+.

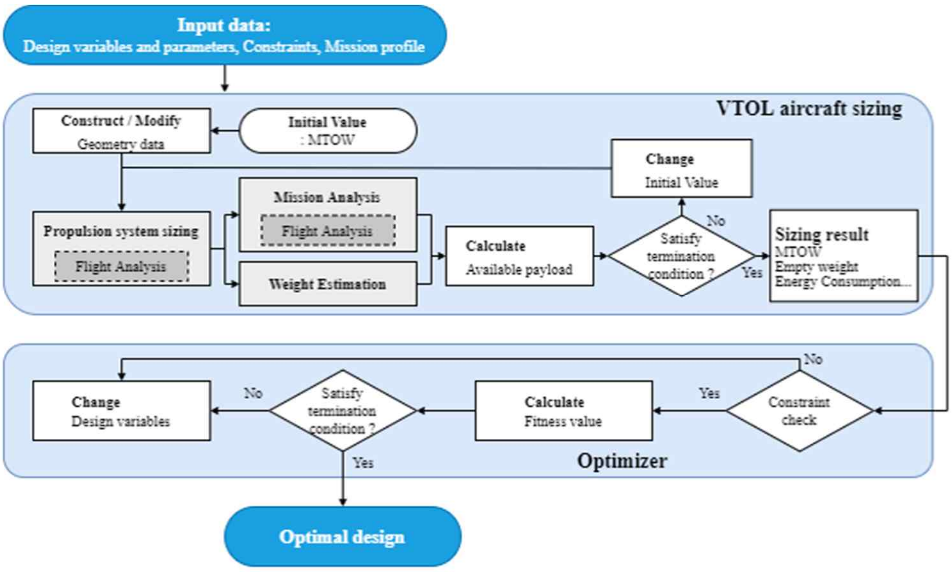

Figure 3. Flowchart of RISPECT+

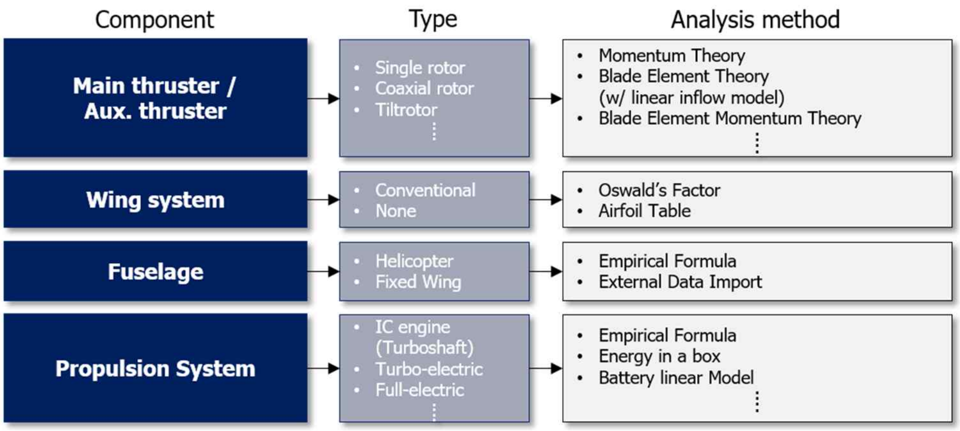

Figure 4. Components and analysis methods considered by RISPECT+

RISPECT+ is largely divided into a sizing process and an optimization process. The sizing process consists of propulsion system sizing, mission profile analysis, flight analysis, and empty weight estimation. Each process is inherently connected, and calculation is performed repeatedly until the convergence conditions are satisfied. In the mission profile analysis stage, based on the propulsion system sizing results, the thrust of each thruster required for the mission and the required fuel consumption are calculated. At this stage, the required thrust and power required for each thruster are calculated through the flight analysis process, which includes analysis modules for thrusters such as rotors and propellers. Figure 4 lists the analysis modules for each component considered in RISPECT+. In the empty weight estimation process, the weight of each component is predicted using the empirical formula based on the input design variables, and it is checked whether the calculated payload value reaches the target payload value. If the payload within the allowable range is derived through the sizing process, feasible ideal design variable combinations can be obtained through a separate optimization process.

2.2. Weight estimation formula for a coaxial rotor with lift−offset maneuver

In the case of a compound helicopter with a lift−offset coaxial rotor, there is an advantage in efficiency in forward flight compared to a conventional coaxial rotor, however, it has a disadvantage in that its weight is designed to be heavy. This is because when designing a lift−offset compound helicopter, it is essential to design a blade that is more rigid than the conventional one and a hub that can withstand a certain level of roll moment. For this reason, there is a limit to using the weight estimation formula built based on the conventional single rotor in order to design a compound helicopter to which lift−offset is applied. Additionally, variables such as tip clearance and tip separation of the coaxial rotor should be considered when estimating the weight. In this study, by referring to the research of Johnson, 2009[15], a weight estimation module considering a lift−offset coaxial rotor was added to RISPECT+ to carry out the conceptual design.

Table 1 lists the weight estimation formula used to estimate the weight of a lift−offset compound helicopter. If the rotor is operated in a lift−offset maneuver, a rigid blade is necessary because it must withstand severe vibration and load. It is for this reason that the weight in the blade weight estimation formula is proportional to the cube of the blade radius. In order to verify the weight estimation module considering a lift−offset coaxial rotor, the weight estimation results of the XH−59A were compared with actual specifications[16]. The thesis of Johnson, 2012[13] was referred to for the value of the technology factor and design variables required for weight estimation used in the process. Figure 6 shows the weight of each component of the actual XH−59A, as well as the results calculated by the improved weight estimation module. The error between the actual weight and the calculated weight was confirmed to be within a valid range with an average error of around 10%, which enabled the weight estimation module to be verified considering the lift−offset compound helicopter.

Table 1. Weight estimation formula for lift-offset compound helicopter

Group	Component	Estimation formula
Structure	Thruster	$W_{rotor} = W_b + W_{hub} + W_{spin}$ $W_{blade} = N_{rotor}\ 0.000083770\omega LR^3/(2(h-s)t_{.2R}^2)$ $W_{hub} = N_{rotor}\ (0.17153\omega R + 0.000010534(W_{blade}\ /N_{rotor}\ )V_{tip}^2\ t_{.2R}^2/R)$ $W_{shaft} = N_{rotor}\ 0.081304\omega LR^2 2h/t_{.2R}^2$
	Horizontal tail	$W_{ht} = 0.7176 S_{HT} AR_{HT}^{0.3173}$
	Vertical tail	$W_{vt} = 1.046 S_{VT} AR_{VT}^{0.5332}$
	Wing	$W_{wing} = 0.036 S_{\omega}^{0.758}\lambda_{\omega}^{0.04}(1.5GW)^{0.49}\left(\frac{AR_{\omega}}{\cos^2(\lambda_{\omega})}\right)^{0.6}\left(\frac{100}{\cos(\lambda_{\omega})c}\right)^{-0.3}$
	Landing gear	$W_{lg} = 0.038GW$
	Fuselage	$W_{fuselage} = 0.8 \times 0.02665 \times 0.76 \times GW^{0.943} R^{0.654}$
Propulsion	Engine	$W_{drg,eng} = 9.277 HP_{MCP}^{0.5365}\ GW^{-0.01035}$
	Gearbox -coaxial	$W_{xmsn} = 1.3 \times 0.172(Q_{max})^{0.8}$
	Gearbox -propeller	$W_{amsn,aux} = 0.172(Q_{max})^{0.8}$
	propeller	$W_{prop} = 0.6 \times 9.035 N_{aux} N_b^{-0.486}\ RPM_{aux}^{-0.459}\ R_{aux}^{0.157}\left(\frac{P_{max,aux}}{N_{fan}}\right)^{0.92}$

parameter	definition	units
N_{rotor}	number of rotors	
N_{blade}	number of blades per rotor	
W_{SD}	structural design gross weight	lb
n_z	design ultimate flight load factor at W_{SD}	g
λ	blade taper ratio (tip chord/root chord)	
$\tau_{.2R}$	blade airfoil thickness-to-chord ratio (at 20%R)	
R	rotor radius	ft
c	blade mean chord	ft
h	coaxial rotor separation (fraction rotor diameter)	
s	coaxial rotor tip clearance (fraction rotor diameter)	
L	lift offset (M_{roll}/TR)	
V_{tip}	rotor hover tip velocity	ft/sec

Figure 5. Parameters used in lift-offset weight estimation formula[17]

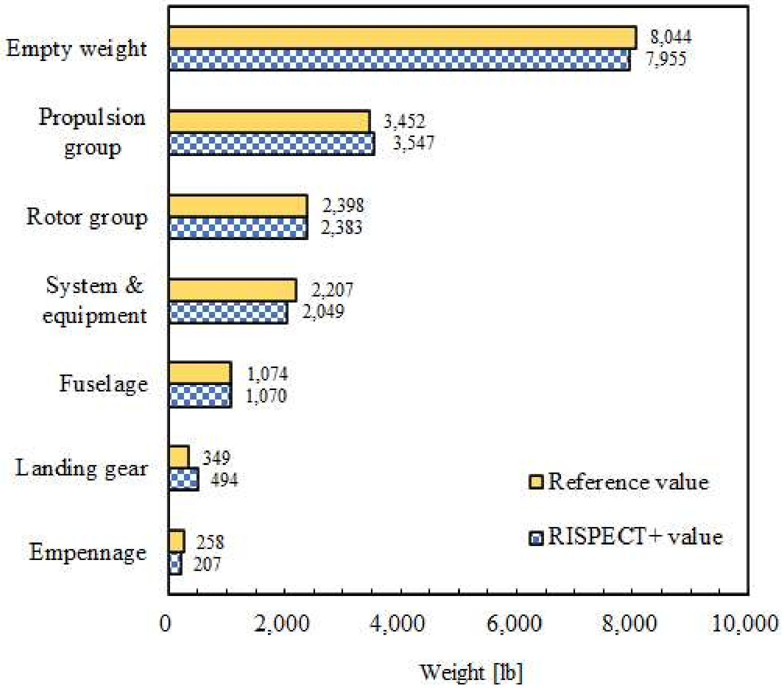

Figure 6. Verification result of Lift-Offset XH-59A weight estimation formula

2.3. Modified Flight Analysis Module

2.3.1. Blade element theory for a lift−offset coaxial rotor

In this study, the conceptual design of a compound helicopter with a lift−offset coaxial rotor was performed by modifying the flight analysis module included in RISPECT+'s propulsion system sizing and mission profile analysis. In this process, RISPECT+ applies momentum theory, blade element momentum theory, and blade element theory to calculate the aerodynamic force of thrusters. In particular, in the case of the main rotor, the blade element theory is used to calculate the thrust coefficient and induced inflow in each rotor during forward flight. However, since the conventional blade element theory was built based on a single rotor and propeller, it should be modified to consider the interference effect of the upper and lower rotors for lift−offset coaxial rotor analysis. Yuan, 2020[18] modified the blade element theory and conducted a coaxial rotor aerodynamic analysis study to take into account the interference effect. This was applied to this study and the conceptual design.

$$\begin{Bmatrix} v_{i_u} = v_u + K_u v_u \frac{r}{R} \cos \psi_u \\ v_{i_l} = v_l + K_l v_l \frac{r}{R} \cos \psi_l \end{Bmatrix} \quad (a)$$

$$\begin{Bmatrix} v_{i_u} = v_u + \delta_u v_l + (K_u v_u + K_l \delta_u v_l) \frac{r}{R} \cos \psi_u \\ v_{i_l} = v_l + \delta_l v_u + (K_l v_l + K_u \delta_l v_u) \frac{r}{R} \cos \psi_l \end{Bmatrix} \quad (b)$$

K_u, K_l : *Pitt & Peters linear inflow model coefficients*

v_{i_u}, v_{i_l} : *axial induced velocity,* v_u, v_l :*uniform induced velocity*

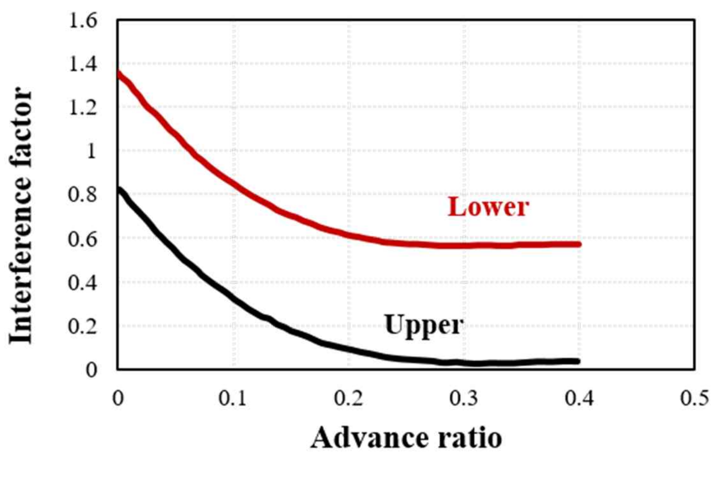

Figure 7. Interference factor along advance ratio[19]

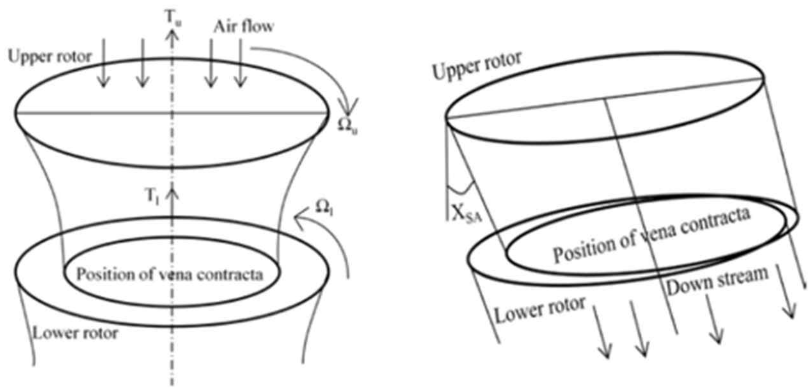

Figure 8. Simplified wake geometry of coaxial rotor[20]

Equation (a) is the linear inflow model of Pitt and Peters used in blade element theory. In the lift-offset coaxial rotor analysis module, the induced velocity was calculated as in equation (b) using an interference factor[19], which means the interference effect between the upper and lower rotors. The interference factor used is shown in Figure 7. It was derived by comparing the results of predicting the performance of the rotor with blade element theory and the prediction using computational fluid analysis. If both interference factors are zero, then equation (b) is equal to equation (a). It is the same as the interference between the two rotors is not taken into account, and the induced velocity for two simple single rotors is calculated. In an actual coaxial rotor, however, the wake generated in the upper rotor accelerates the velocity of inflow flowing into the lower rotor. Additionally, due to the suction effect caused by the rotation of the lower rotor, the induced velocity of the upper rotor also becomes larger than that of the single rotor. Therefore, to include the interference effect of the upper and lower rotors, the change in induced velocity of the coaxial rotor was calculated by adding a positive interference factor as shown in equation (b). Also, looking at Figure 7, it can be seen that the interference factor decreases as the advance ratio increases. This is because the skew angle, which is the direction in a rotor's wake moves, gradually increases as the advance ratio increases. As shown in Figure 8, as the skew angle increases, the area in a plane of the lower rotor affected by the wake of the upper rotor decreases. Therefore, the interference factor decreases as the advance ratio increases. When the advance ratio exceeds 0.3, the skew angle converges to 90 degrees, thus the wake occurs almost flat with the rotor plane, and the induced velocities of the upper and lower rotors converge to zero[21]. In conclusion, if the advance ratio is 0.3 or more, the interference factor is calculated as $\delta_u \cong 0$ and $\delta_l \cong 0.6$, respectively.

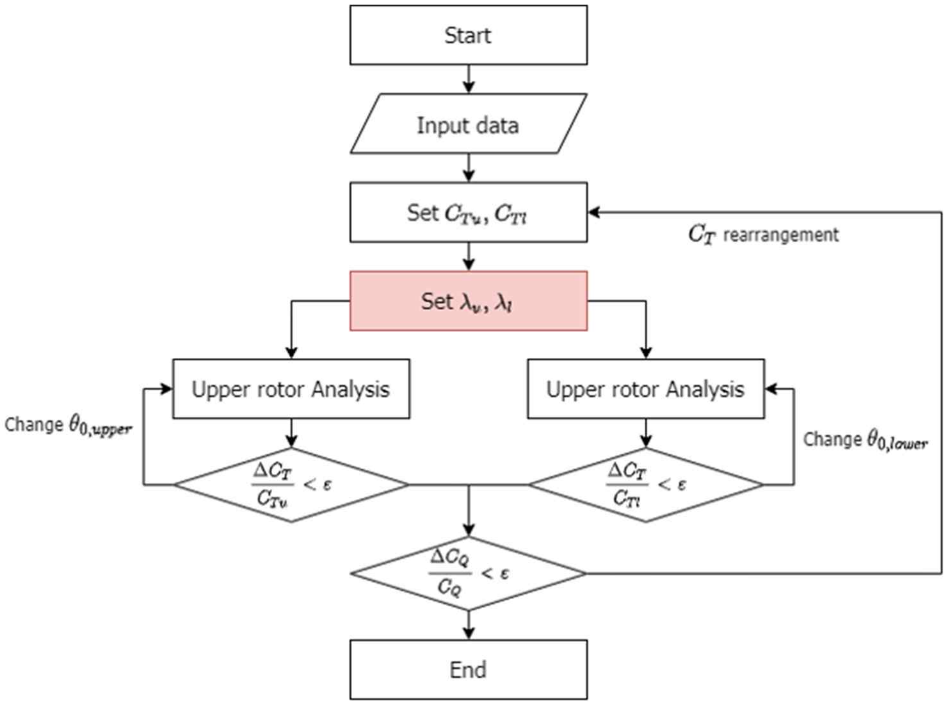

Figure 9. Flowchart of a lift-offset coaxial rotor analysis module

A flow chart of a lift-offset coaxial rotor analysis module using the modified linear inflow model is shown in Figure 9. Since a thrust demanded for a lift-offset coaxial rotor system is generated by a combination of the upper and lower rotors, the demanded thrust is first randomly distributed to the upper and lower rotors. Then, the blade-element theory is applied to the upper and lower rotors respectively to find the pitch angle that can generate the distributed thrust. After that, to balance the torque between the upper and lower rotors, it is checked whether a trim condition is satisfied. If the trim condition is not satisfied, the thrust is redistributed and the same process is repeated until the trim condition is satisfied. In this process, constraints were set so that the pitch angle of each rotor was not excessively increased by more than 30 degrees, and the thrust distribution ratio of the lower rotor to the upper rotor was not excessively deflected to less than 30% or greater than 70%.

$$LOS = \frac{\Delta M_x}{TR} \approx 0.8\mu^2 \tag{c}$$

$$\theta_{1c,LOS} = \theta_{1c} + \left(\beta_{1s} - C_{M_x}\right)/\gamma(-\nu_\beta^2 - 1 - 1.5e) \tag{d}$$

Equation (c) calculates the LOS (Lift-Offset) value, which means the lateral position of the center of lift on each rotor surface. ΔM_x is the difference in roll moment between the upper and lower rotors, T is the sum of thrust generated by the two rotors, and R means the rotor radius. When the rotor is in lift-offset maneuver by assigning a LOS value to the rotor, the roll moment value to be generated in each of the upper and lower rotors is determined by equation (c). The lift-offset coaxial rotor analysis module calculates the corresponding roll moment value. That value affects the determination of the cyclic pitch of each rotor within the iteration of the convergence of the pitch angle as shown in equation (d). θ_{1c} means the lateral cyclic pitch angle when a rotor is not in lift-offset maneuver and is calculated using the formula developed in the research by Chopra, 2017[22]. In equation (d), γ and ν_β mean lock number and flapping frequency, respectively.

2.3.2. Validation cases

To verify the developed lift-offset coaxial rotor analysis module, the results of the Harrington rotor wind tunnel test by Dingeldein, 1954[23][24] and the XH-59A test flight[25] were used. First, except for the lift-offset maneuver, Harrington rotor 1 was analyzed to confirm that the analysis module included the interference effect between the upper and lower rotors of the coaxial rotor sufficiently. The verification specifications are shown in Table 2, and the required power according to the advance ratio was calculated using blades with airfoil arranged as shown in Figure 10. The Harrington rotor consists of about 8 airfoils, and the aerodynamic data for each airfoil was used by constructing the C81 Table for each angle and Mach number using KFLOW[26], an in-house CFD code. In addition, additional verification of induced, profile, and parasite power was performed through CAMRAD II. The structure of the rotor blade was modeled as a rigid body, and the lift line theory and the free wake model were used for the unsteady aerodynamic load of the rotor blade. For the analysis of a stall, a static stall model was used, and the unsteady flow was modeled using the ONERA-EDLIN model. The azimuth angle step was set to 2 degrees. blades were analyzed by dividing each into 17 parts in the span direction. The trim target was set so that torque, pitch moment, and roll moment of the upper and lower rotors were zero. A collective pitch angle and a cyclic pitch angle of the upper and lower rotors were set as trim variables. The shaft angle was determined by referring to the thesis of Barbely [27].

Table 2. Specifications of Harrington rotor 1

Parameter	Harrington rotor 1
Radius	12.5 ft
No. of blades (per rotor)	2
Taper	0.39
Solidity (Coaxial)	0.054
Twist	None

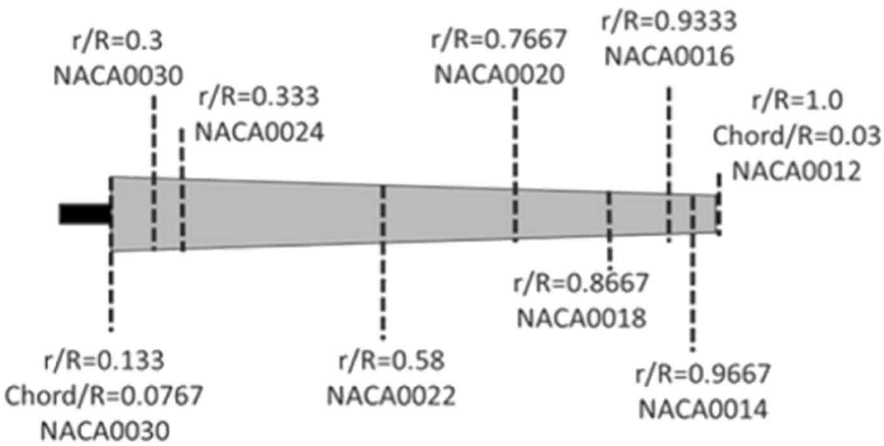

Figure 10. Arrangement of the airfoils (Harrington rotor 1)[28]

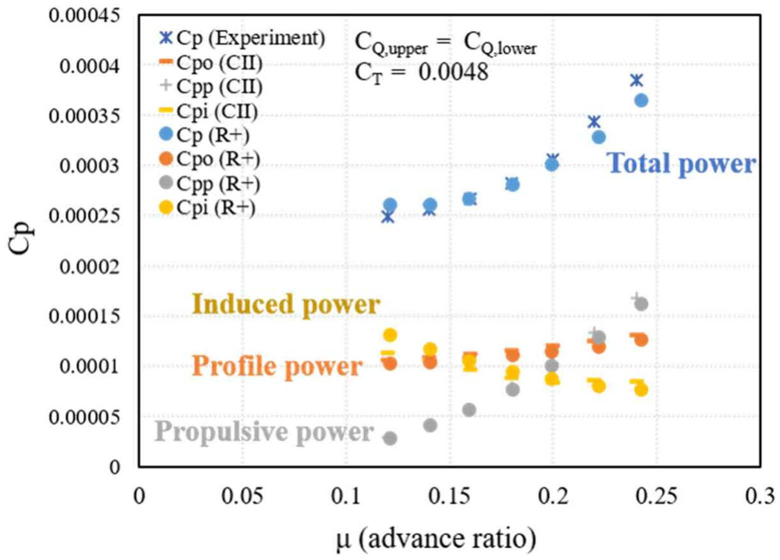

Figure 11. Comparison of required power according to advance ratio

The required power according to the advance ratio of the Harrington rotor 1 using the lift-offset coaxial rotor analysis module and CAMRAD II is shown in Figure 11, and the experimental results are also displayed. It can be confirmed that the total required power is predicted similarly by both the experiment and the two analysis methods, and the profile power and parasite power are also consistent with results of CAMRAD II. Especially, the induced inflow could be calculated by considering the blade crossover effect and the effect of the wake from the upper rotor on the lower rotor, which were difficult to include in the conventional blade element theory method based on a simple single rotor. As a result, it can be confirmed that the required power estimation result calculated through the improved rotor analysis module agrees with the result of

CAMRAD II.

In addition, through comparison with the flight test results of the XH−59A, it was verified that the improved rotor analysis module produced appropriate results when the lift−offset maneuver was added to the rotor. The verification specifications are shown in Table 3, and the analysis was performed using the airfoil arrangement diagram provided in the appendix of the thesis written by Jacobellis, 2018[29]. Figure 13 is a graph showing the required power of the compound helicopter according to the forward flight speed, and the flight test results, RCAS (Rotorcraft Comprehensive Analysis System) analysis results[25], and the analysis results with the improved lift−offset coaxial rotor analysis module are displayed together. The flight test results shown in Figure 13 are the required power when the auxiliary thruster is operated together when the forward flight speed is 100 knots or more. Comparing the results, it can be seen that the required power can be predicted within a valid range through the improved rotor analysis module, with an average error of about 13% from the flight test result and an average error of about 9% from the RCAS analysis result. Based on these two verification cases, it was judged that the developed lift−offset coaxial rotor analysis module was suitable for use in a conceptual design of a lift−offset compound helicopter.

Table 3. Specifications of XH-59A rotor

Parameter	Rotor of XH-59A
Radius	18 ft
No. of blades (per rotor)	3
Taper	0.5
Solidity (Coaxial)	0.127

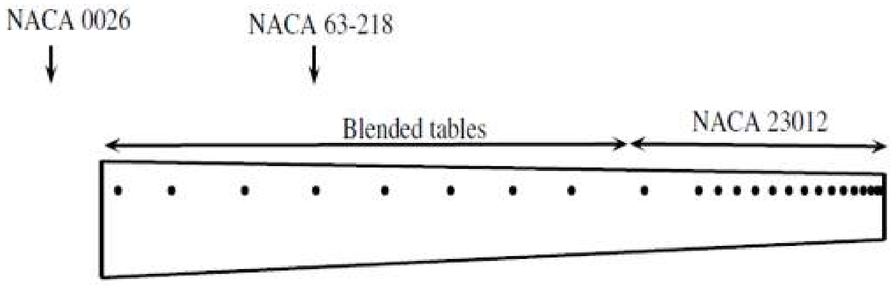

Figure 12. Arrangement of the airfoils (XH-59A)[29]

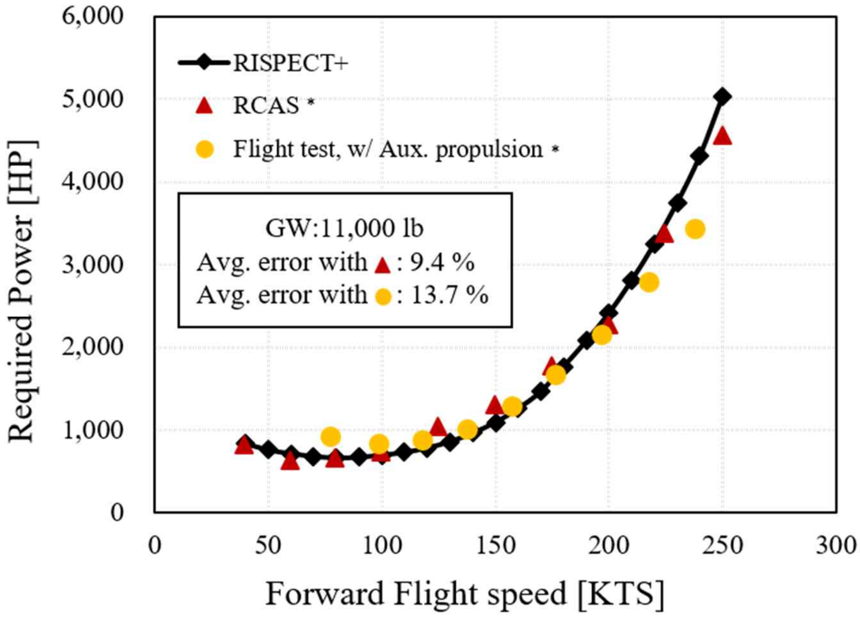

Figure 13. Comparison of required power according to forward flight speed (*[25])

2.4. Initial Conceptual design results

2.4.1. Mission profile

Initial sizing was calculated using the conceptual design process described above to obtain the configuration information of the lift−offset compound helicopter that uses lift−offset maneuvers in high−speed forward flight. the military mission proposed by Johnson, 2012[13] was used as the mission profile. Figure 14 is a simplified diagram of the mission profile. Specific mission conditions are indicated in Johnson, 2012[13]. In the conceptual design, the SB>1 defiant including a lift−offset coaxial main rotor and one pusher propeller as an auxiliary thruster was used as a reference. In addition, a payload of 6,600 lb including 2 flight attendants, and 2 cabin crew was specified as a design requirement. Furthermore, the maximum forward speed should be 230 knots. The mission profile includes high-speed forward flight at an altitude of 14,000 ft and uses a lift-offset maneuver of about 0.25 for climbing and forward flight missions. Hovering and loitering missions account for more than 20% of the total mission time. Therefore, the lift-offset compound helicopter's forward flight performance as well as its hovering performance can be considered simultaneously.

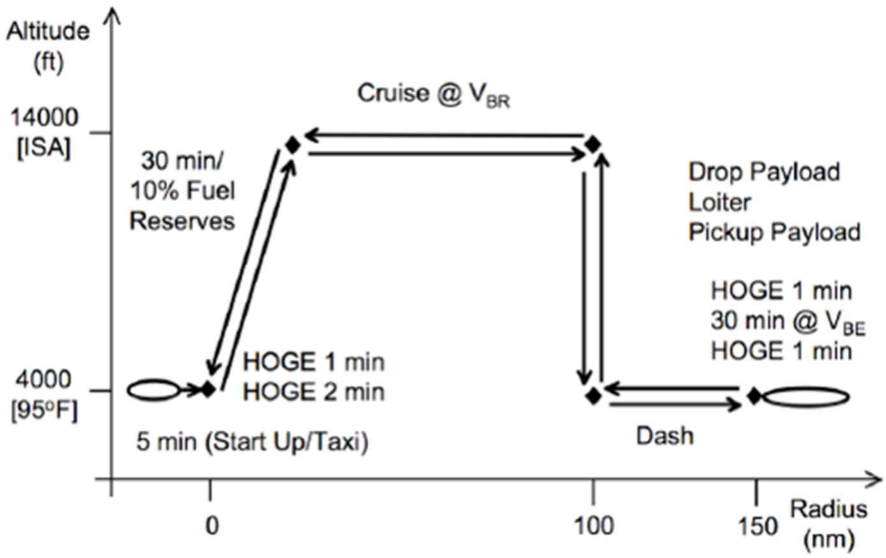

Figure 14. The mission profile for lift-offset compound helicopter[13]

2.4.2. Sizing, Weight, and Required power estimation results

Figure 15 is the lift−offset compound helicopter configuration drawn based on the initial sizing results. The length of the upper and lower rotor blades is 23.8 ft, the chord length is 2.1 ft, and the aspect ratio is about 11.3. As a result of initial sizing, the maximum tip Mach number on the advancing side is about 0.89, which is similar to the maximum tip Mach number of 0.9 on the advancing side of the X2[30]. Also, the radius of the pusher propeller that supplies an additional thrust during forward flight is designed to be 6.9ft.

In addition, Figure 16 shows the calculated weight estimation result, and as a result of the conceptual design, the estimated total weight of the lift−offset compound helicopter is about 33,400 lb. The component that occupies the largest proportion of the empty weight of the designed helicopter is the lift−offset coaxial rotor, which accounts for about 38.6% of the total empty weight. In the case of blades used for a lift−offset coaxial rotor, a very robust design should be in progress because they have to withstand large vibrations caused by lift−offset maneuvers. Additionally, since the rotor hub is designed to withstand a certain level of roll moment generated in each of the upper and lower rotors, it is estimated to be heavier than the weight of a hub used in a conventional single−rotor helicopter. This tendency coincides with the fact that the rotor weight is calculated in proportion to the cube of the rotor radius in the weight estimation formula. The empty weight ratio to the total weight of the designed lift-offset compound helicopter is about 58.8%. In the case of the XH-59A aircraft, which first applied the lift-offset maneuver, the empty weight ratio to the total weight is known to be about 55.4%[16]. Since the total weight difference between the XH-59A and the helicopter designed in this study is about 3 times, the empty weight ratio to the total weight of the designed aircraft can be considered a valid result.

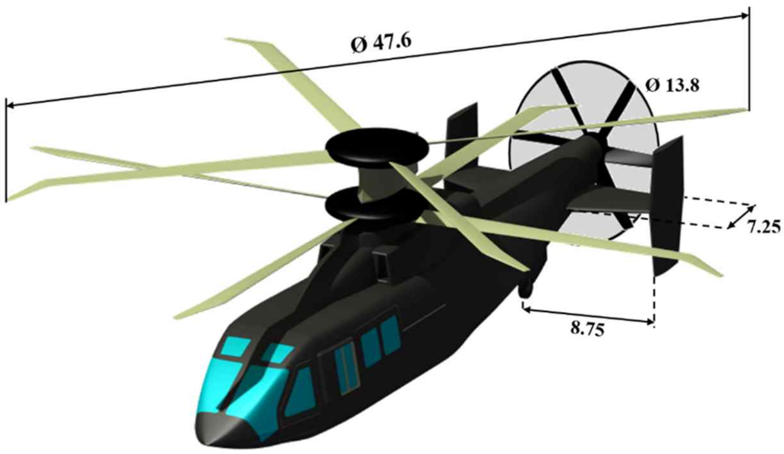

Figure 15. Sizing results of conceptual design (unit : ft)

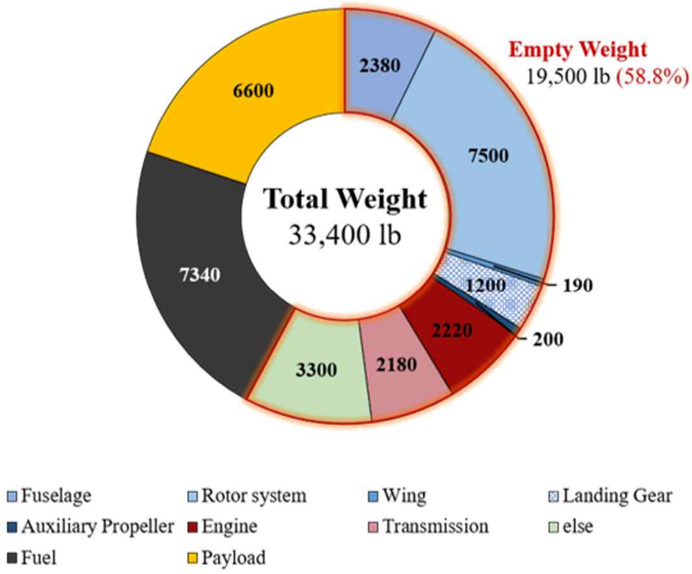

Figure 16. Weight estimation results of components

Figure 17 is a schematic diagram of fuel consumption and required power estimation results according to mission performance. It can be seen that the largest power is required during high-speed forward flight, which is due to the large parasite drag generated from the fuselage and hub. Thus, the propulsion engine sizing was carried out based on the required power during high-speed forward flight, and it was assumed that the lift-offset compound helicopter uses a total of two engines. As a result, the maximum power of the engine was about 10,500 HP, and the MCP (Maximum Continuous Power) of one engine was calculated to be about 4,640 HP. Analyzing the result of calculating the required power according to the mission, the total required power equals that of the rotor because the pusher propeller is not driven during hovering. However, during high-speed forward flight, it was confirmed that the required power of the pusher propeller was 3,140HP, accounting for about 48% of the total required power.

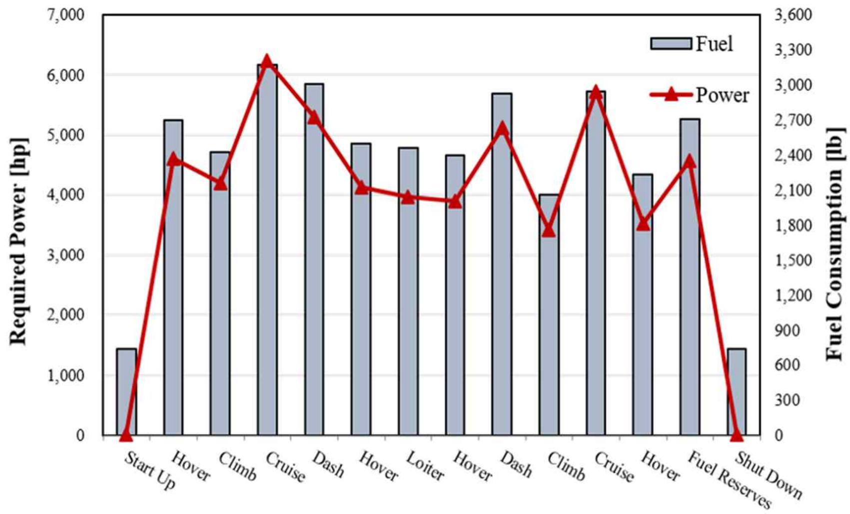

Figure 17. Changes in required power and fuel consumption as the mission progresses

As a result of the initial sizing, it was confirmed that the aerodynamic performance of the lift-offset coaxial rotor greatly affects the weight and required power of the compound helicopter. It was confirmed that the specifications of the lift-offset coaxial rotor not only have a very direct effect on the rotor weight, which accounts for about 40% of the empty weight but also have a significant effect on the calculation of the required power that affects the sizing of the propulsion engine. Therefore, in this study, the aerodynamic performance improvement of the rotor was additionally considered in the conceptual design stage by continuing the airfoil design process of the rotor blade. Through this process, it has been possible to quantify how the lift-offset coaxial rotor's aerodynamic performance affects the conceptual design of the compound helicopter.

Chapter 3. Airfoil design process

3.1. Analysis of a lift−offset coaxial rotor aerodynamic performance

Results of the lift−offset coaxial rotor analysis module, which was used for rotor performance analysis during conceptual design, were analyzed to derive the design conditions required for airfoil design used in blades. The analysis was conducted based on two missions: hovering and high−speed forward flight. The time required for each mission in hovering and high−speed forward flight takes up more than 20% of the total mission time, respectively, and the aerodynamic characteristics of the rotors during the two missions are very different. In hovering, a lift−offset maneuver is not used, and the wake generated from the upper rotor propagates in the direction of the rotational axis, greatly affecting the lower rotor. On the other hand, in high−speed forward flight, a lift−offset maneuver is used, and the wake generated in the upper rotor has a rather insignificant effect on the lower rotor because the wake is propagated in a direction parallel to the rotor plane due to a large advance ratio. Therefore, in this study, the aerodynamic characteristics of the rotor during the two missions were analyzed, respectively, and research was conducted to include that results in airfoil design.

Approximately 21% of the 160−minute total mission time is devoted to the hover mission, which takes 35 minutes. During hovering, the slowdown condition, which reduces the rotational speed of the rotor according to forward speed, is not applied. At this time, the rotor blade tip rotational speed is 630 ft/s, approximately 0.55 Mach. Figure 18 shows the sectional lift and lift coefficient distribution of the upper and lower rotors according to the radius of the rotor during hovering. Consequently, it can be confirmed that the lower rotor is greatly affected by the influence of the wake of the upper rotor. Up to about 80% of the rotor radius from the root, a sufficient lift is not generated due to a strong downwash occurring in the upper rotor. This is because the wake generated in the upper rotor propagates downward and simultaneously contracts, affecting up to around r/R = 0.8 in the lower rotor.

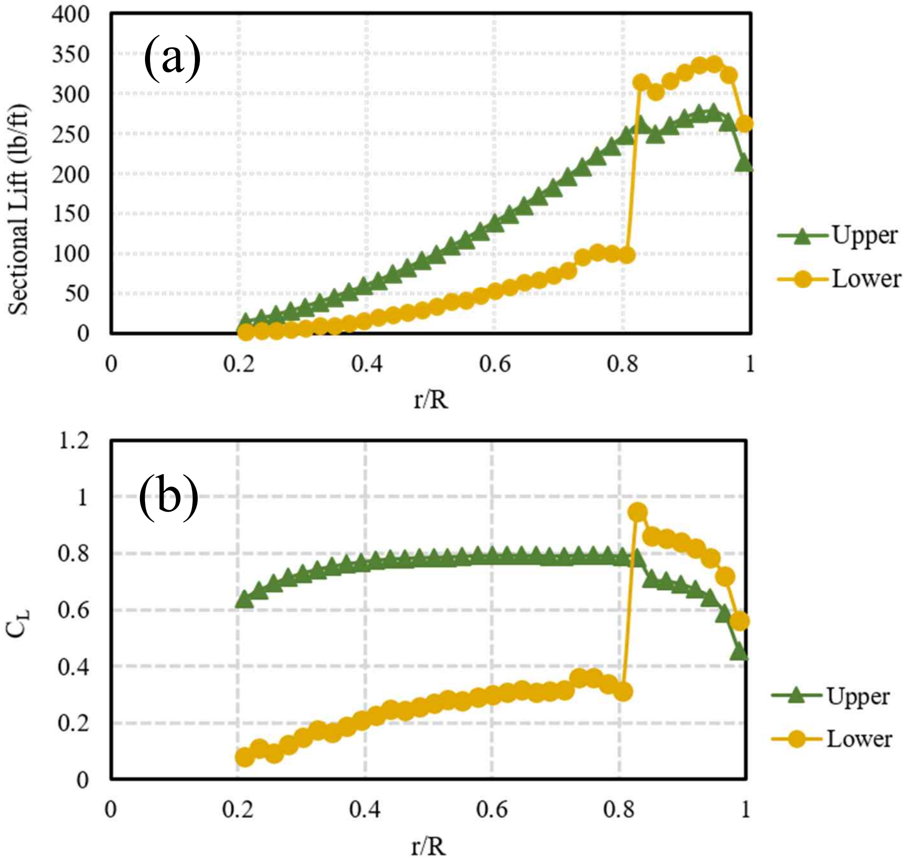

Figure 18. Distribution of (a) sectional lift and (b) lift coefficient at hovering

The high-speed forward flight lasts about 70 minutes out of a 160-minute total mission time. In high-speed forward flight, a slowdown condition that reduces the rotor rotational speed according to forward speed is applied to prevent the generation of shock at the tip of the rotor blades. Based on the forward speed of 220 knots, the rotor blade tip Mach number applied with the slowdown condition is about 0.83 and the advance ratio is about 0.63. Moreover, in order to achieve high efficiency during high-speed forward flight, a lift-offset maneuver is used to operate the rotor and LOS of about 0.25 is given. Figure 19 and Figure 20 show the distribution of sectional lift and effective angle of attack on the upper and lower rotor during high−speed forward flight. Most of the lift is generated on the advancing side, and the lift−offset rotor has a nearly symmetrical distribution of lift generated from the upper and lower rotors. Since the advance ratio is at a very high level of 0.6 or more, it can also be confirmed that the reverse flow area is very large.

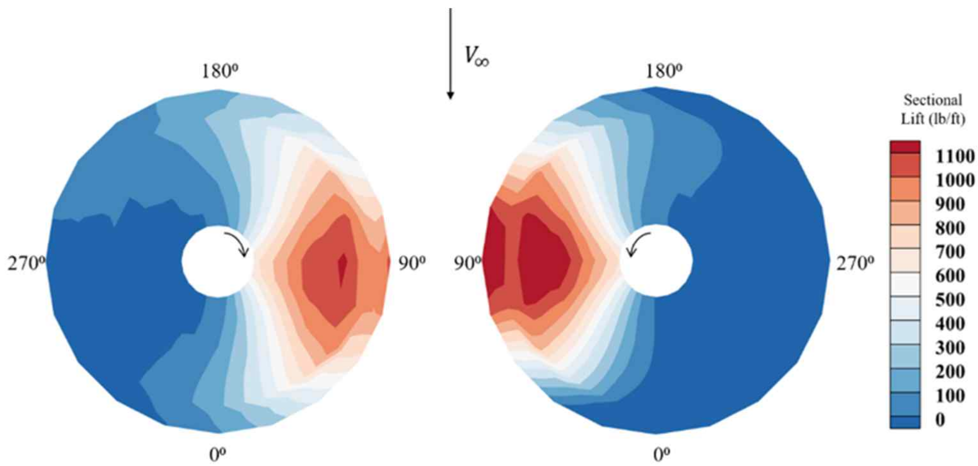

Figure 19. Contours of sectional lift at high-speed forward flight

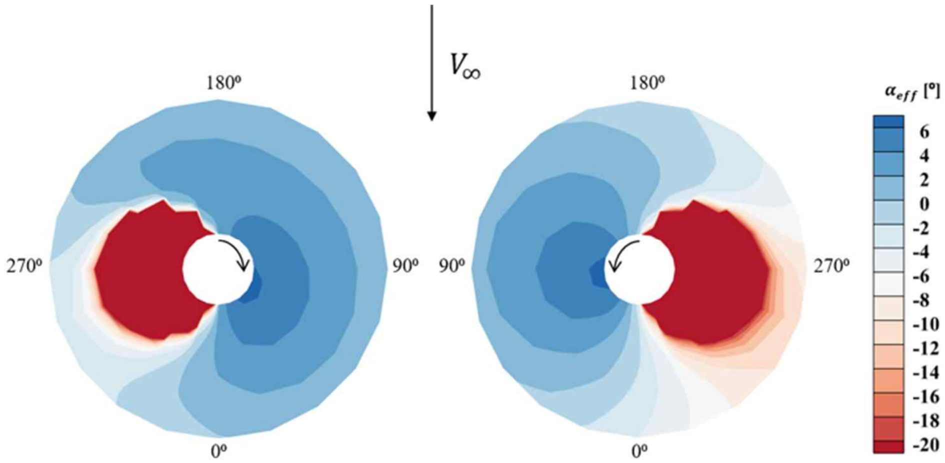

Figure 20. Contours of effective angle of attack at forward flight

Based on the results of the aerodynamic analysis in hovering and high-speed forward flight, the airfoil design was carried out by dividing a blade into three parts as shown in Figure 22. A blade in Figure 22 is the configuration derived from conceptual design results, and VR7 and VR8 airfoils were used for initial sizing. When hovering, up to the point where the radius of the blade is around 80% from the root is within the sphere of influence of the upper rotor's wake. Furthermore, as can be seen in Figure 21, which shows the distribution of the lift coefficient in the upper rotor during high-speed forward flight, the lift force distribution pattern on the advancing side during high-speed flight changes at the point where the radius of the blade is around 7 to 80% from the root. Therefore, the point where the radius of the blade is 80% from the root was designated as the branching point dividing mid-board and out-board regions of the blade, and airfoils applied to mid−board and out−board were designed respectively.

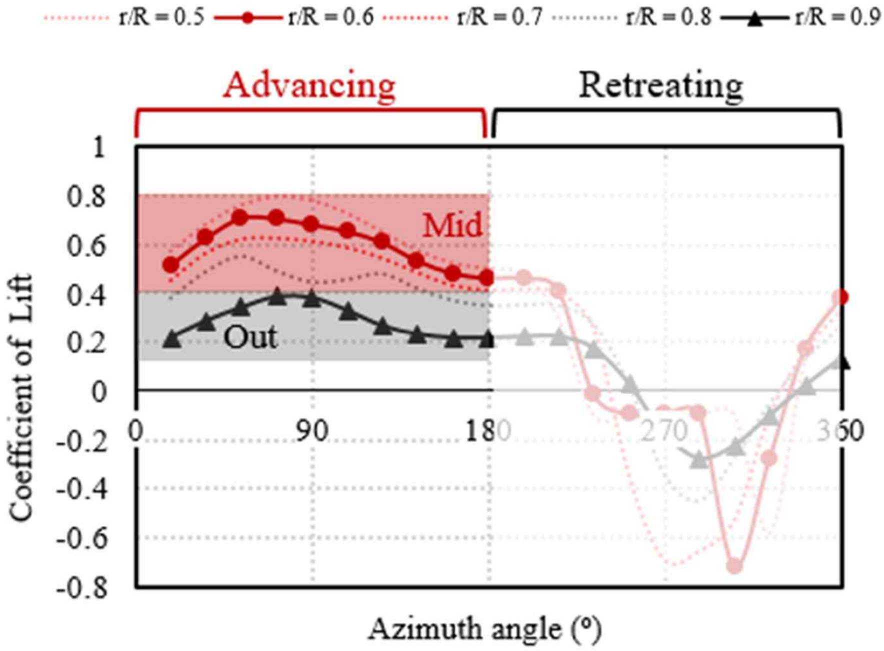

Figure 21. Lift coefficient distribution in forward flight

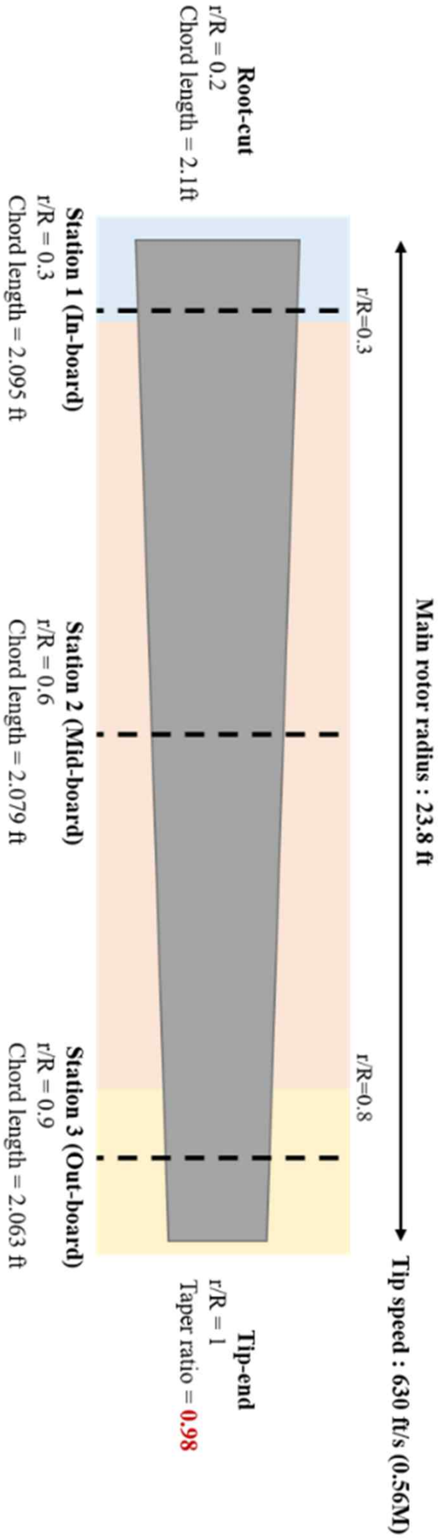

Figure 22. Conceptual design geometry result of the rotor blade

3.2. A framework for airfoil design

In this study, a framework for blade airfoil design was built in-house using Python. The framework was created using DEAP[31], which is a Python library for genetic algorithms, and XFOIL aerodynamic analysis program[32], which was created by strongly combining the panel method and Euler equation with the integrated boundary layer equation. DEAP library contains several single-objective and multi-objective optimization algorithms. In this study, optimization was performed using NSGA-II[33], which is a multi-objective function optimization algorithm. Since XFOIL has excellent calculation speed, it is suitable for optimization design programs that need to analyze a large amount of data in a short time. However, since there is a disadvantage that the reliability of analysis accuracy is somewhat lower in high Reynolds flow region, an aerodynamic analysis was additionally performed using KFLOW, an in-house CFD code, after the airfoil design was completed. The developed airfoil shape design framework was built to enable parallel optimization using SCOOP[34]. Through this, evaluation can be made quickly by dividing the number population defined by a user for a genetic algorithm by the number of allocated CPU cores.

3.2.1. Airfoil Parameterization method

An airfoil parameterization function method used for airfoil design is IGP (Improved Geometric Parameter) method[35]. This method has the advantage of being able to designate an airfoil using 8 design variables which are fewer than those of PARSEC[36], CST(Class Shape Transformation)[37], and OBF(Orthogonal Basis Function) method[38]. PARSEC and CST use 11 design variables to create an airfoil. OBF uses 10 design variables. Also, since design variables are related to the aerodynamic characteristics of an airfoil, such as leading-edge radius and maximum thickness, it is easy to define a design space. The IGP method separates a camber-line and a thickness-line to determine an airfoil. First, a camber-line is determined using a cubic Bezier curve as equation (e).

$$\begin{aligned} x_c &= 3c_1 k(1-k)^2 + 3c_2(1-k)k^2 + k^3 \\ y_c &= 3c_3 k(1-k)^2 + 3c_4(1-k)k^2 \end{aligned} \qquad (e)$$

x_c and y_c mean x, y coordinates of a camber-line, respectively. k, an independent variable varies from 0 to 1 to determine x_c and y_c. In the above equation, c_1, c_2, c_3, and c_4 are design variables for determining a camber-line. A thickness-line is specified in the following equation by applying the thickness curve basis function of the NACA "four-digit" airfoil series.

$$\begin{cases} t_1 X_T^{0.5} + t_2 X_T + t_3 X_T^2 + t_4 X_T^3 + t_5 X_T^4 = T \\ 0.5 t_1 X_T^{-0.5} + t_2 + 2t_3 X_T + 2t_3 X_T + 3t_4 X_T^2 + 4t_5 X_T^3 = 0 \\ 0.25 t_1 + 0.5 t_2 + t_3 + 1.5 t_4 + 2t_5 = -\tan \beta_{TE}/2 \\ t_1 = \sqrt{2\rho_0} \\ t_1 + t_2 + t_3 + t_4 + t_5 = 0 \end{cases} \qquad (f)$$

$$t = t_1 x^{0.5} + t_2 x + t_3 x^2 + t_4 x^3 + t_5 x^4 \qquad (g)$$

In equation (f), T means a maximum thickness, and X_T means x coordinate where the maximum thickness is located in an airfoil. β_{TE} is a boat−tail angle of the trailing edge, which is a design variable related to the thickness of the trailing edge. ρ_0 is a leading−edge radius. if four design variables(T, X_T, β_{TE}, ρ_0) are specified, Values of t_1, t_2, t_3, t_4 and t_5 that determine a thickness−line can be derived through equation (f). By substituting these five values into equation (g), airfoil thickness according to x coordinate can be specified.

In this study, the modified IGP method[39] was used for airfoil design to obtain optimization design results rapidly by removing unnecessary design space and reducing design variables. This method is proposed by modifying the equation used for determining a camber−line in the IGP method. When specifying a camber−line, the method used by the NACA “three−digit” series was applied rather than simply using the cubic Bezier curve. NACA “three−digit” series includes NACA23012, which is often used for a helicopter. NACA “three−digit” series uses the following camber−line equation.

$$\frac{y}{c}=\frac{k_1}{6}\left[\left(\frac{x}{c}\right)^3-3r\left(\frac{x}{c}\right)^2+r^2(3-r)\frac{x}{c}\right]\ from\quad \frac{x}{c}=0\ to\ r$$
$$\frac{y}{c}=\frac{k_1r^3}{6}\left(1-\frac{x}{c}\right)\ from\quad \frac{x}{c}=r\ to\ 1 \qquad (h)$$

In equation (h), r means a chord-wise location for the zero value of the second derivative of the three-digit camber-line equation. k_1 is a value designated to obtain a specific lift coefficient. The modified IGP method does not use c_1, c_2, c_3, and c_4 as design variables for determining a camber-line, but uses two design variables, r, and k_1.

3.2.2. Objectives and Constraints for airfoil design

The purpose of airfoil design in the conceptual design stage is to reduce the required power, which affects engine sizing and weight estimation. This is done by improving the aerodynamic performance of the lift-offset coaxial rotor which accounts for about 40% of the empty weight. The aerodynamic performance of the rotor was improved by specifying an objective to minimize the drag coefficient of an airfoil used for blades. Objectives were designated as Equation (i) by calculating the average drag coefficient during hovering and high-speed forward flight missions. In equation (i), the average drag coefficient ($c_{d,mean}$) was derived through the lift-offset coaxial rotor analysis module developed through this study.

$$obj_1 = c_{d,hover,mean} / c_{d,hover,ref}$$
$$obj_2 = c_{d,forward,mean} / c_{d,forward,ref} \quad (i)$$

To calculate the average drag coefficient, the drag coefficient (c_d) was calculated in the range of the lift coefficient (c_l). That range is derived based on aerodynamic performance results at the advancing side of an upper rotor during the mission. The range of lift coefficient calculated for each mission is shown in Table 4. The calculated drag coefficient was interpolated with a modified Akima spline for deriving an average drag coefficient. In equation (i), reference values of the average drag coefficient for each mission ($c_{d,hovering,ref}$, $c_{d,forward,ref}$) are indicated. That values were derived by analyzing VR7 and VR8 airfoils used in the conceptual design stage. By including the two values in objectives, a degree of improvement compared to an airfoil's aerodynamic performance used in a conceptual design was used as an index for airfoil design.

Table 4. Flow conditions for airfoil design

12% Mid-	Mach number	Re× 10^6	c_l range
Hovering	0.34	5.0	0.6 … 0.8
Forward flight	0.64	9.4	0.4 … 0.8
8% Out-	Mach number	Re× 10^6	c_l range
Hovering	0.51	7.4	0.4 … 0.8
Forward flight	0.80	11.7	0.2 … 0.4

$$con_1 = c_{l,max} > 0.9 \times c_{l,max,reference}$$
$$con_2 = \left|c_{m,0}\right| < constant \qquad (j)$$

Additionally, in this study, a ratio of a maximum airfoil thickness to a chord length was given as a constraint considering a structural design of a blade. In the case of airfoils used in a mid-board region of a blade, the ratio of a maximum airfoil thickness to a chord length was 12%, and in the case of airfoils used in an out-board region of a blade, that constraint was set to be 8%. For reference, the ratio of a maximum airfoil thickness to a chord length of VR7 and VR8 used in the conceptual design is 12.0% and 8.1%, respectively. Furthermore, a second constraint was imposed so that a maximum lift coefficient ($c_{l,max}$) of an airfoil to be designed was 90% or more of a maximum lift coefficient ($c_{l,max,reference}$) of the airfoil used in the conceptual design. Through these constraints, it is possible to prevent a decrease in stall margin due to a decrease in drag. Lift coefficients were calculated according to a change in an angle of attack under flow conditions in Table 4, and a maximum value was derived after interpolating the three largest values among them using a quadratic interpolation polynomial. Finally, a third constraint was imposed so that an absolute value of a zero lift pitching moment coefficient ($c_{m,0}$)

of an airfoil to be designed was less than 0.02 in the mid-board region and 0.03 or less in the out-board region[39]. This constraint is to prevent an airfoil to be designed from having an excessively high pitching moment.

3.3. Results of Airfoil design at Conceptual design stage

3.3.1. Designed Airfoil for mid and out-board region of the blade

The airfoil applied to the mid-board region of a blade was designed as shown in Figure 23. Also, through an airfoil design process, pareto fronts like Figure 24 were obtained. Analyzing the pareto fronts, it can be seen that shapes with lower maximum camber were mainly selected. However, since lowering a maximum camber directly affects a reduction of a lift coefficient, it was confirmed that most infeasible points occurred because they did not satisfy constraints related to a maximum lift coefficient. In this study, the shape with the highest lift coefficient among shapes of the pareto front was selected as a final design point. This is to generate a similar thrust when the designed airfoil is applied to rotors compared to when the VR7 airfoil used in the conceptual design is applied to rotors, and, at the same time, to bring a reduction in the required rotor power. In addition, in the process of selecting a final design point, an airfoil shape with a thin trailing edge was excluded. If a boat tail angle was less than 10º, it was judged to be a thin trailing edge. This is because, when a trailing edge is too thin, not only difficulties rise in manufacturing, but also structural breakage easily occurs.

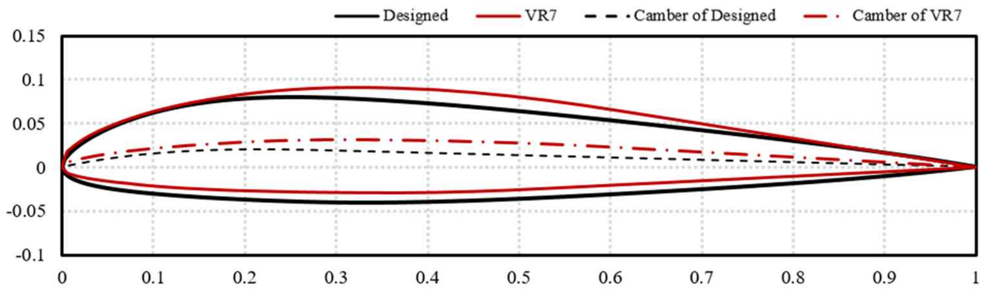

Figure 23. Geometry comparison of designed and baseline airfoil for the mid-board region

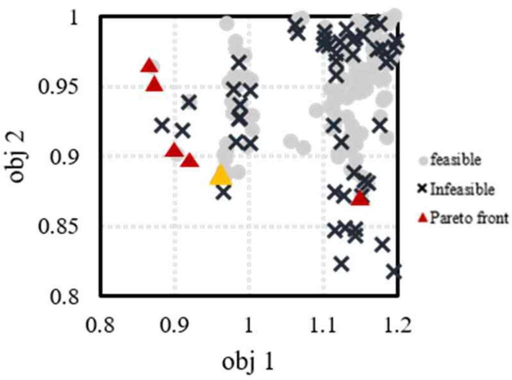

Figure 24. Pareto fronts obtained during airfoil design for the mid-board region

Figure 25 is the airfoil design result applied to the out-board region of a blade derived through an airfoil design process. Looking at Figure 26, the distribution of pareto fronts for two objectives, drag reduction during hovering and drag reduction during high-speed forward flight, and the distribution of feasible and infeasible points analyzed in the optimization process can be seen. Analyzing pareto fronts, it can be seen that shapes with thin trailing edges were mainly selected to reduce drag. However, as described above, when a trailing edge is too thin, not only difficulties rise in manufacturing, but also structural breakage is likely to occur. Therefore, in this study, among pareto front shapes, the shape with the largest boat tail angle which means the thickest trailing edge was selected as the final design point. Comparing the shape selected as a final design point and VR8 airfoil used as a baseline, a position of maximum thickness was located at about 33% from a leading edge in the case of VR8 and about 29% in the case of the designed airfoil.

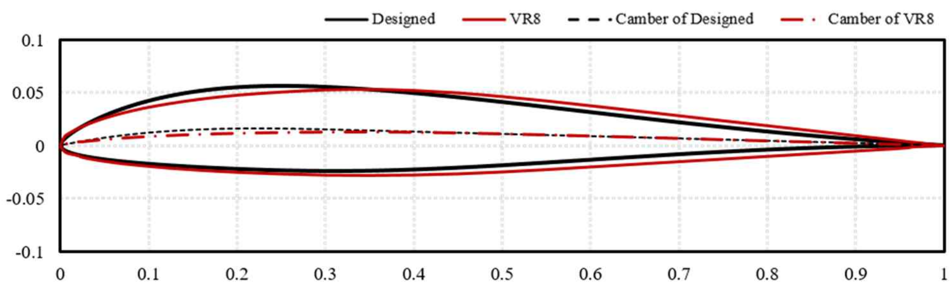

Figure 25. Geometry comparison of designed and baseline airfoil for the out-board region

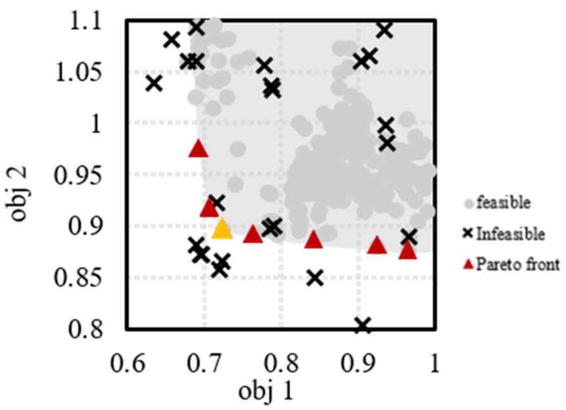

Figure 26. Pareto fronts obtained during airfoil design for the out-board region

The results of airfoil analysis using XFOIL, which is an aerodynamic analysis program used in the airfoil design framework, are shown in Figure 27 and Figure 28. Moreover, in order to obtain reliable aerodynamic performance information for designed airfoils, additional analysis was conducted using KFLOW, an in-house CFD code, and the results are shown in Figure 29 and Figure 30. As conditions of CFD, the analysis was performed considering an altitude of 0 ft, an air density of 1.225 kg/m^3, and a viscosity of 1.789×10^{-5} kg/m/s. Each airfoil was analyzed using an O-grid type two-dimensional grid, and the number of each grid was about 30,000. Far-boundary grids were placed 30 times a chord length away from an airfoil so that a boundary condition did not affect a calculation result of an airfoil's aerodynamic performance. Compressible, steady two-dimensional Reynolds Averaged Navier-Stokes (RANS) equation was used as a governing equation, and $k-\omega$ turbulence model and $\gamma - Re_\theta$ transition model were used for turbulence analysis. The highlighted parts in Figure 29 and Figure 30 mean a range of lift coefficients on the advancing side during the mission derived through the improved rotor analysis module.

side during the mission derived through the improved rotor analysis module.

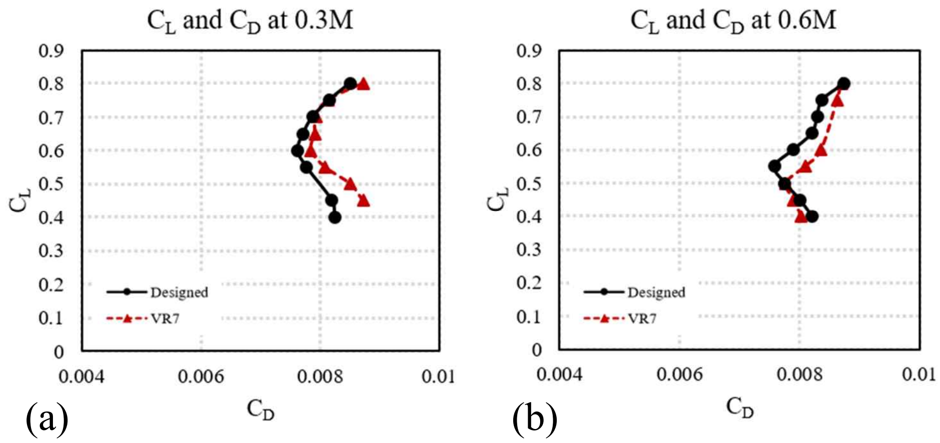

Figure 27. Lift-Drag polar of airfoils for the mid-board region calculated by XFOIL at (a) Hovering and (b) Forward Flight

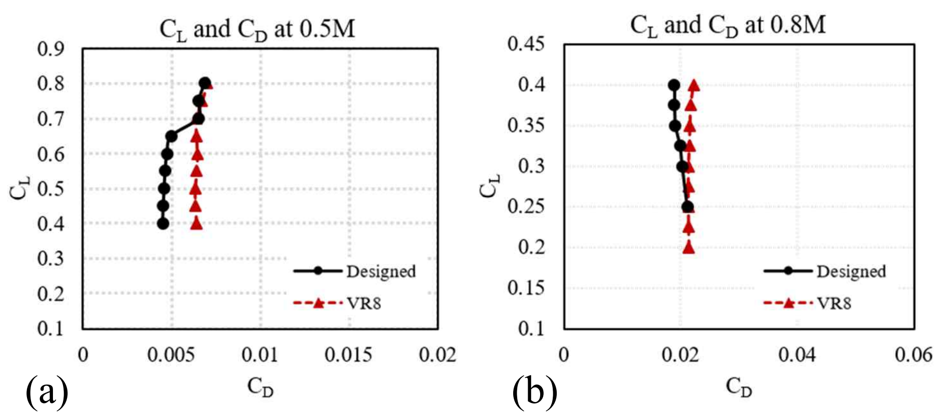

Figure 28. Lift-Drag polar of airfoils for the out-board region calculated by XFOIL at (a) Hovering and (b) Forward Flight

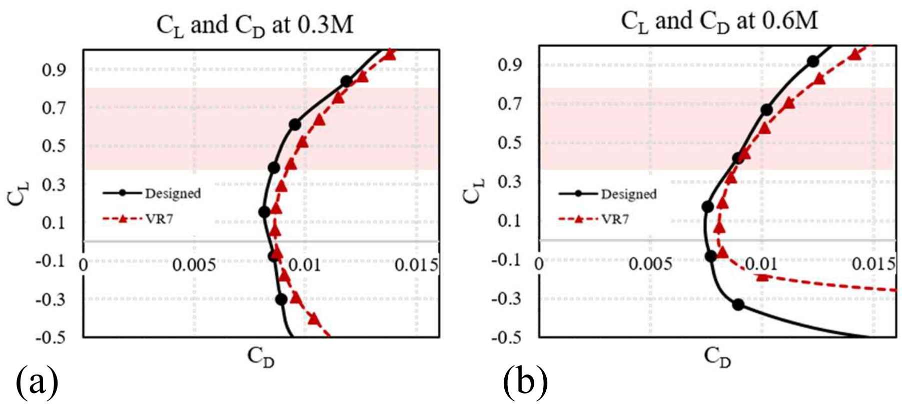

Figure 29. Lift-Drag polar of airfoils for the mid-board region calculated by in-house CFD code KFLOW at (a) Hovering and (b) Forward Flight

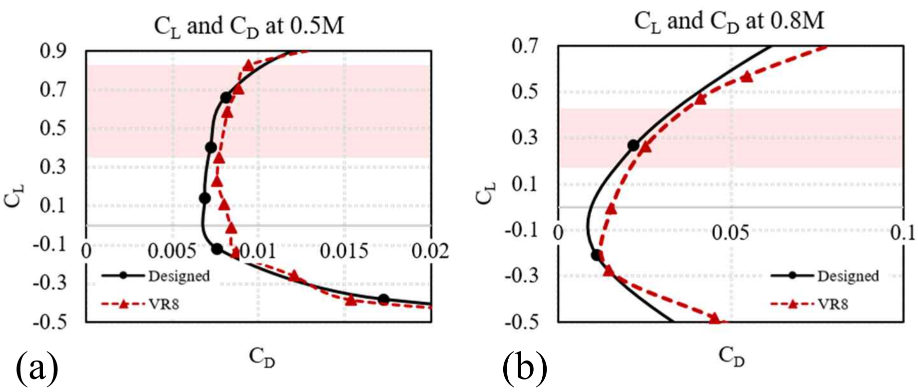

Figure 30. Lift-Drag polar of airfoils for the out-board region calculated by in-house CFD code KFLOW at (a) Hovering and (b) Forward Flight

Comparing the figures, it can be confirmed that the designed airfoil improved the drag coefficient compared to the baseline airfoil. In the case of the airfoil designed to be applied to the mid-board region of blades, as a result of analysis with XFOIL, it can be confirmed that the average drag coefficient decreased by about 3.9% at 0.3 Mach and by about 12.3% at 0.6 Mach. These results show the same tendency as when interpreted by in-house CFD code KFLOW.

The mean drag coefficient in the range of lift coefficients is reduced by about 5.3% and about 8.8% at 0.3 Mach and 0.6 Mach, respectively. For the airfoil designed to be applied to the out-board region of blades, according to XFOIL analysis, the average drag coefficient decreased by about 11.8% at 0.5 Mach, and by about 6.7% at 0.8 Mach. These results also show the same tendency as when interpreted by in-house CFD code KFLOW. The average drag coefficient in the range of lift was reduced by about 7.9% and about 4.7% at 0.5 Mach and 0.8 Mach, respectively.

3.3.2. Results of Conceptual design with Designed Airfoils

Designed airfoils were applied again to a conceptual design process of a lift-offset compound helicopter to obtain improved conceptual design results. Before proceeding with a conceptual design, a performance of a rotor was analyzed based on the design results using baseline airfoils. Through this process, it was confirmed how much the aerodynamic characteristics of designed airfoils affect the performance of a rotor. When a conceptual design was carried out using baseline airfoils, the length of a blade was about 23.8 ft, and a taper ratio of 0.98 and a linear twist of −8 degrees were applied to a blade. When blades of the same specification are used, information on rotor thrust, required power, and figure of merit can be found in Figure 31. When designed airfoils were applied, the required power required to generate the same thrust was reduced by about 8%. Rotor's figure of merit was also improved by about 9%. In other words, by applying airfoil design at the conceptual design stage, there was room for additional weight and sizing optimization.

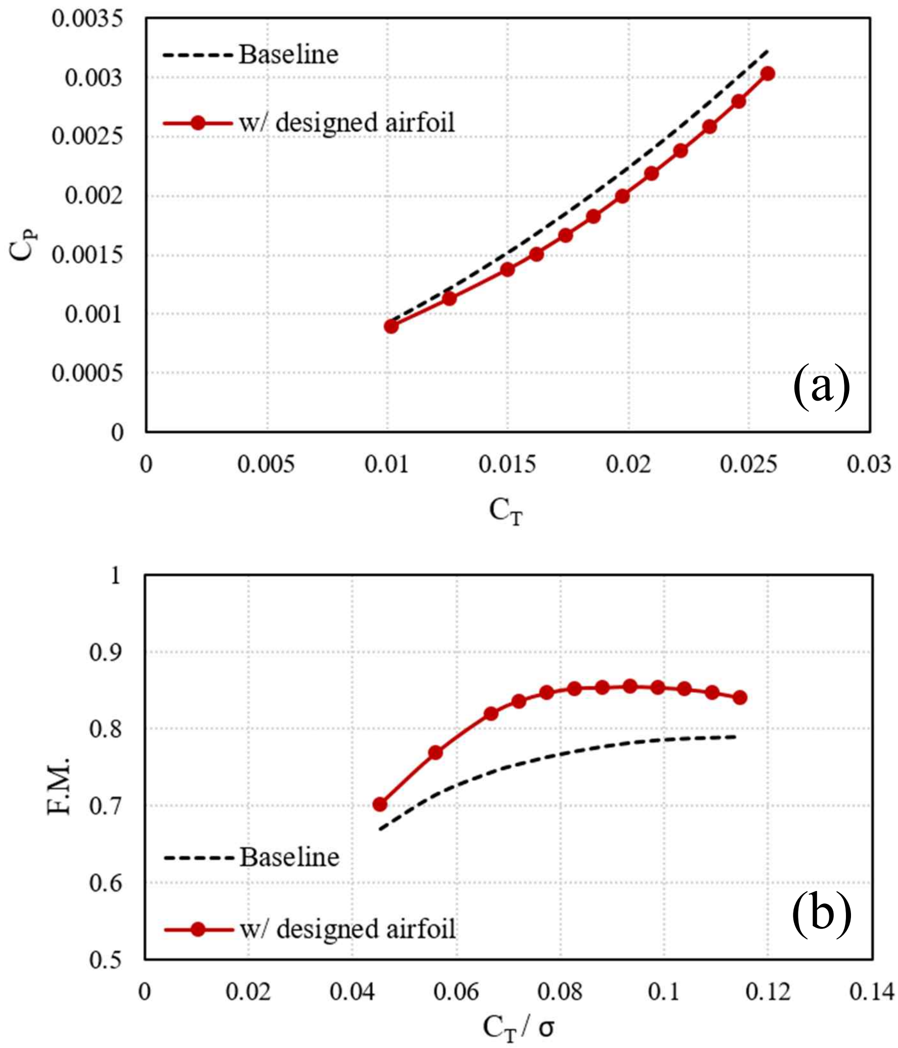

Figure 31. Comparisons of (a) power coefficient and (b) figure of merit when designed airfoils are applied

The conceptual design process previously conducted was repeated by applying designed airfoils. The mission profile and design requirements used are the same as in the previous conceptual design process. Figure 32 and Figure 33 indicate the sizing and weight estimation results of the lift-offset compound helicopter derived from the conceptual design results. The results confirmed a lift-offset coaxial rotor and pusher-propeller with reduced radii. The rotor radius decreased by about 2.1% from 23.8 ft to 23.3 ft, and the propeller radius decreased by about 4.3% from 6.9 ft to 6.6 ft. The biggest reason for these results is that increased rotor blade airfoil aerodynamic performance, as confirmed in Figure 31, triggered a reduction of a rotor blade radius. Also, because rotor weight is proportional to the cube of a rotor radius, rotor weight, and empty weight are reduced. Therefore, due to the reduced weight, and reduced propeller required power during high-speed flight, the propeller radius is also reduced. Nevertheless, the proportion of empty weights remains at 60% of gross weight. Plus, the item that occupies the largest part of the empty weight is the weight of the lift-offset coaxial rotor.

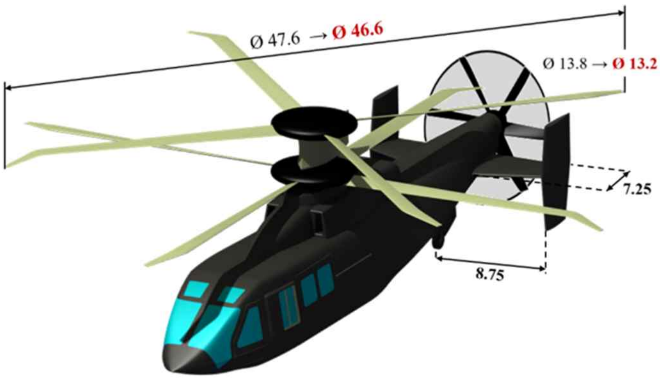

Figure 32. Sizing results of conceptual design with designed airfoils (unit : ft)

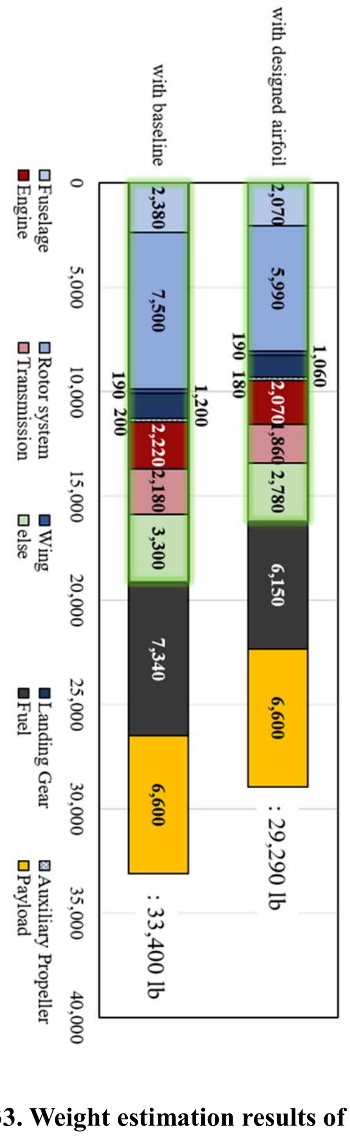

Figure 33. Weight estimation results of components

The effect of improving aerodynamic characteristics of airfoils can also be confirmed by estimated fuel consumption and required power as shown in Figure 34 calculated as a result of the conceptual design. It can be seen that the total required power is reduced because the rotor weight and total weight are reduced due to the improved rotor performance. In particular, power for a rotor of 4,540 HP was required when baseline airfoils were used for hovering mission, but power for a rotor of 3,540 HP was required when designed airfoils were used, resulting in a reduction of about 22.0%. In addition, power for a rotor of 3,580 HP was required when baseline airfoils were used for high-speed forward flight missions, but power for a rotor of 3,080 HP was required when designed airfoils were used, resulting in a reduction of about 13.9%. In Figure 31, which confirmed the performance of the rotor, the reduction in required power for the same thrust was about 8%, but the reduction effect of more than 8% in each mission was because the weight of other parts was reduced. The reduction in the required rotor radius and weight made a snowball effect for decreasing each component. Another thing to note is that the effect of reducing the required power was greater in high-speed forward flight than in hovering. The cause of this phenomenon is that a pusher-propeller does not operate during hovering. However, the required power of a pusher-propeller accounts for about 42% and the ratio of the required power of the rotor to the total required power is relatively low during high-speed forward flight missions. Therefore, this result appeared because the influence of a propeller required power was greater during high-speed forward flight than during hovering.

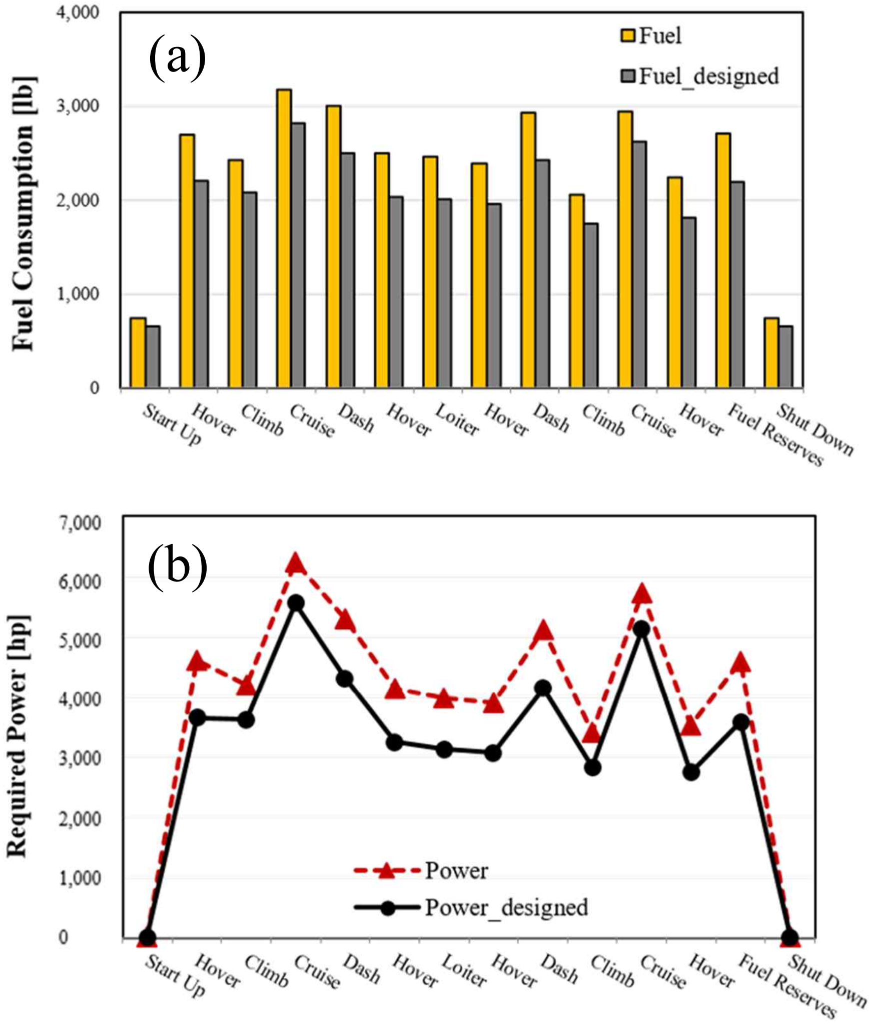

Figure 34. Comparison of (a) fuel consumption and (b) required power

Chapter 4. Conclusions

In this study, by modifying a blade−element theory, a lift−offset coaxial rotor analysis module and a weight estimation module for a lift−offset compound helicopter were established and based on this, the conceptual design process for a lift−offset compound helicopter was summarized. Using the established conceptual design process, initial sizing was performed for the mission profile to perform high−speed forward flight with a maximum forward speed of 220 knots using lift−offset maneuvers. As a result, it was confirmed that the lift−offset coaxial rotor accounted for about 40% of the empty weight of the compound helicopter and that the highest required power of 6,720 HP was required during high−speed forward flight in the overall mission profile. Therefore, an increase in the aerodynamic performance of blades would not only improve a rotor's weight and size, but would also greatly impact a compound helicopter's weight, size, and required power. Thus, an airfoil design of a rotor blade was additionally carried out, and an effect of the rotor’s aerodynamic performance on the conceptual design result of the lift−offset compound helicopter was quantitatively investigated by including it in a conceptual design stage.

In the case of a lift−offset coaxial rotor, unlike a conventional single rotor, a complicated flow phenomenon occurs due to an interference effect of upper and lower rotors. In this study, it is possible to reduce cost and time compared to high−fidelity tools such as CAMRAD II and CFD by analyzing the aerodynamic characteristics of a rotor with the improved lift−offset coaxial rotor analysis module that can be used in a conceptual design stage and using it for airfoil design. As a result of the analysis, a region in which a lower rotor was affected by the wake generated by an upper rotor occurred during hovering. In addition, during forward flight, it was confirmed that most of the lift was generated on the advancing side of a rotor using lift−offset maneuver, and the distribution of lift generation on the upper and lower rotor plane was symmetrical. Considering these results, flow conditions for airfoil design were selected by dividing a rotor blade into three sections. The IGP method was used for deciding a configuration of an airfoil. After performing the optimization design process using the NSGA−II algorithm and XFOIL, an improved conceptual design result was derived by applying designed airfoils.

As a result of the improved conceptual design, the rotor radius was reduced by about 2.1%, and the total weight of the lift−offset compound helicopter was reduced by about 12.3%. In addition, it was confirmed that the required power reduction effect was 22.0% and

13.9%, respectively, during hovering mission and forward flight mission. Through this process, by using the improved lift-offset coaxial rotor analysis module, the disadvantages of high-fidelity tools that it is inappropriate to use in the concept design stage in terms of cost and time could be overcome. Plus, it was confirmed that the results of the rotor analysis module could be used for airfoil design to derive improved conceptual design results.

Bibliography

[1] [1] Milton A. Schwartzberg, Dr.Roger L. Smith, James L.Means, Dr. Harold Y. H. Law, David P. Chappell, “Single-Rotor Helicopter Design and Performance Estimation Programs, Volume 1, Methodology”, U.S. Army Air Mobility R&D Laboratory, SRIO Report Number 77-1, 1977.

[2] Johnson, Wayne. Rotorcraft aeromechanics. Vol. 36. Cambridge University Press, 2013.

[3] Go, Jeong-In, Do-Hyung Kim, and Jae-Sang Park. "Performance and vibration analyses of lift-offset helicopters." International Journal of Aerospace Engineering 2017 (2017).

[4] Ruddell, A. J., Groth, W., & McCutcheon, R. Advancing blade concept (ABC) technology demonstrator. UNITED TECHNOLOGIES CORP STRATFORD CT SIKORSKY AIRCRAFT DIV. 1981

[5] Ford, Aaron. Helicopter Dynamics Concerning Retreating Blade Stall on a Coaxial Helicopter. Diss. San José State University, 2019.

[6] Gertler, Jeremiah. "Army Future Vertical Lift (FVL) Program." LIBRARY OF CONGRESS WASHINGTON DC, 2020.

[7] Blackwell, R., & Millott, T. Dynamics design characteristics of the Sikorsky X2 technology™ demonstrator aircraft. annual forum proceedings-American Helicopter Society. Vol. 64. No. 1. American Helicopter Society, Inc, 2008.

[8] Trimble, Stephen. "Sikorsky unveils S-97 for high-speed scout and attack helo". Flightglobal, 20 October 2010.

[9] Johnson, Wayne. "Rotorcraft Aeromechanics Applications of a Comprehensive Analysis,” Presented at Heli Japan 98." AHS International Meeting on Advanced Rotorcraft Technology and Disaster Relief. 1998.

[10] Feil, Roland, et al. "Aeromechanics analysis of a high-advance-ratio lift-offset coaxial

rotor system." Journal of Aircraft 56.1 (2019): 166-178.

[11] Kwon, Young-Min, et al. "Aeromechanics analyses of a modern lift-offset coaxial rotor in high-speed forward flight." International Journal of Aeronautical and Space Sciences 22.2 (2021): 338-351.

[12] Yeo, Hyeonsoo, and Wayne Johnson. "Investigation of maximum blade loading capability of lift-offset rotors." Journal of the American Helicopter Society 59.1 (2014): 1-12.

[13] Johnson, Wayne, Alex M. Moodie, and Hyeonsoo Yeo. Design and performance of lift-offset rotorcraft for short-haul missions. National Aeronautics and Space Administration Moffett Field Ca Ames Research Center, 2012.

[14] Lee, D., Lim, D., and Yee, K., Generic Design Methodology for Vertical Takeoff and Landing Aircraft with Hybrid-Electric Propulsion, Journal of Aircraft, 59.2, 2022, 278-292.

[15] Johnson, Wayne, and Aeromechanics Branch. "NDARC NASA Design and Analysis of Rotorcraft, Theory." Release 1.0, NASA Ames Research. 2009.

[16] Go, Jeong-In, Jae-Sang Park, and Jong-Soo Choi. "Validation on conceptual design and performance analyses for compound rotorcrafts considering lift-offset." International Journal of Aeronautical and Space Sciences 18.1 (2017): 154-164.

[17] Johnson, Wayne. NDARC NASA design and analysis of rotorcraft. No. ARC-E-DAA-TN46522. 2017.

[18] Yuan, Ye, D. Thomson, and R. Chen. "Variable rotor speed strategy for coaxial compound helicopters with lift–offset rotors." The Aeronautical Journal 124.1271 (2020): 96-120.

[19] Zhang, Yonghua, et al. "Aerodynamic Performance Evaluation of XH-59A Helicopter Rotor in Forward Flight." AIAA Propulsion and Energy 2019 Forum. 2019.

[20] Harun-Or-Rashid, Mohammad, et al. "Inflow prediction and first principles modeling of a coaxial rotor unmanned aerial vehicle in forward flight." International Journal of

Aeronautical and Space Sciences 16.4 (2015): 614-623.

[21] Leishman, Gordon J. Principles of helicopter aerodynamics with CD extra. Cambridge university press, 2006.

[22] Chopra, Inderjit. “Helicopter Dynamics and Bearingless Rotor Analysis”, 2017

[23] Dingeldein, Richard C. Wind-tunnel studies of the performance of multirotor configurations. No. 3236. National Advisory Committee for Aeronautics, 1954.

[24] Harun-Or-Rashid, Mohammad, et al. "Inflow prediction and first principles modeling of a coaxial rotor unmanned aerial vehicle in forward flight." International Journal of Aeronautical and Space Sciences 16.4 (2015): 614-623.

[25] Jacobellis, George, Farhan Gandhi, and Matthew Floros. "A physics-based approach to trim optimization of coaxial helicopters in high-speed flight." Proceedings of the American Helicopter Society International 71st Annual Forum. 2015

[26] Kim, Jee Woong, Soo Hyung Park, and Yung Hoon Yu. "Euler and Navier-Stokes simulations of helicopter rotor blade in forward flight using an overlapped grid solver." 19th AIAA Computational Fluid Dynamics. 2009. 4268.

[27] Barbely, Natasha Lydia, and Narayanan M. Komerath. "Coaxial rotor flow phenomena in forward flight." 2016 International Powered Lift Conference (IPLC)/SAE Aerospace Systems and Technology Conference. No. ARC-E-DAA-TN31139. 2016.

[28] Thiele, Moritz, Martin Obster, and Mirko Hornung. "Aerodynamic modeling of coaxial counter-rotating uav propellers." VFS, 8th Biennial Autonomous VTOL Technical Meeting. 2019.

[29] Jacobellis, George. Improvement of High-Speed Coaxial Rotor Performance Using Redundant Controls and Camber Morphing. Rensselaer Polytechnic Institute, 2018.

[30] Hong, Sung Boo, et al. "Active Airframe Vibration Control Simulations of Lift-offset High-Speed Compound Helicopters" The Korean Society for Aeronautical & Space Sciences Conference Abstract book (2021): 234-235.

[31] Fortin, Félix-Antoine, et al. "DEAP: Evolutionary algorithms made easy." The Journal

of Machine Learning Research 13.1 (2012): 2171-2175.

[32] Drela, Mark. "XFOIL: An analysis and design system for low Reynolds number airfoils." Low Reynolds number aerodynamics. Springer, Berlin, Heidelberg, 1989. 1-12.

[33] Deb, Kalyanmoy, et al. "A fast and elitist multiobjective genetic algorithm: NSGA-II." IEEE transactions on evolutionary computation 6.2 (2002): 182-197.

[34] Hold-Geoffroy, Yannick, Olivier Gagnon, and Marc Parizeau. "Once you SCOOP, no need to fork." Proceedings of the 2014 Annual Conference on Extreme Science and Engineering Discovery Environment. 2014.

[35] Lu, Xiaoqiang, et al. "An improved geometric parameter airfoil parameterization method." Aerospace Science and Technology 78 (2018): 241-247.

[36] Sobieczky, Helmut. "Parametric airfoils and wings." Recent development of aerodynamic design methodologies: inverse design and optimization (1999): 71-87.

[37] Kulfan, B. M. "A Universal Parametric Geometry Representation Method–" CST"– 45th AIAA Aerospace Sciences Meeting and Exhibit." (2007).

[38] Robinson, G. M., and A. J. Keane. "Concise orthogonal representation of supercritical airfoils." Journal of Aircraft 38.3 (2001): 580-583.

[39] Wilke, Gunter. "A Numerical Optimization Framework for Rotor Airfoil Design." European Rotorcraft Forum 48th (2022) 051

[40] Ladson, Charles L., et al. “Computer program to obtain ordinates for NACA airfoils.” NASA Langley Research Center, Hampton, Virginia, No. L-17509. 1996.

Abstract in Korean

개념 설계 단계에서의 Lift-Offset 복합형 회전익기 블레이드 형상 설계 연구

Hyojin Kook
Aerospace Engineering
The Graduate School
Seoul National University

후퇴면에서 발생하는 동적 실속으로 인한 고속 전진 비행 시의 낮은 효율은 전통적인 단일 로터 헬리콥터의 개선되기 어려운 단점이다. Lift-offset은 후퇴면에서 양력 손실이 발생하더라도, 전진면에서 발생시킬 수 있는 최대한의 양력을 만들어 고속 전진 비행 시의 효율을 증가시켜 이 단점을 극복할 수 있는 방법이다. 더불어, stiff hingeless rotor의 개발로 단일 로터면에서 불균형한 양력이 발생하여 작지 않은 크기의 롤모멘트가 만들어져도 로터의 구동이 가능해졌다.

하지만 lift-offset 동축반전 로터는 상부와 하부 로터간의 간섭과 같은 복잡한 유동 현상 때문에 CAMRAD II와 전산유체해석으로 대표되는 high-fidelity 방법을 사용하여 분석이 진행되었다. 본 연구에서 저자는 깃-요소 이론을 변형한 lift-offset 동축반전 로터 해석 모듈을 개발하여 수직 이착륙기 사이징 프로그램인 RISPECT+에 적용하였다. 이를 통해, 개념설계 단계에서 적은 시간과 비용으로 lift-

offset 복합형 회전익기를 설계하는 과정을 제안하였다.

제안된 개념 설계 과정을 사용하여 하나의 puhser propeller와 lift-offset 동축반전 로터를 가진 형상의 초기 사이징을 진행하였다. 또한, 추가적으로 개념 설계 단계에서 로터 블레이드의 익형 설계를 진행하고 이를 개념설계에 반영하여 로터의 공력 성능이 lift-offset 복합형 회전익기의 개념설계 결과에 미치는 영향을 정량적으로 알아보고자 하였다. 익형 설계는 로터 블레이드를 세 구간으로 나누어 유동 해석 조건을 선정한 후, IGP 기법을 이용하여 진행되었다. NSGA-II 알고리즘 및 XFOIL을 사용하여 최적화 설계 과정을 수행한 후, 설계된 익형을 적용하여 개선된 개념 설계 결과를 도출하였다. 그 결과 개념 설계 단계에서 개선된 로터 해석 모듈을 이용한 익형 설계를 진행하여 lift-offset 복합형 회전익기의 공허중량과 요구 동력에 큰 영향을 미치는 lift-offset 동축반전 로터에 대한 개선된 설계 결과를 얻을 수 있다는 결론을 도출하였다.

주용어: Lift-offset 동축반전 로터, 개념설계, 로터 블레이드 형상 설계

학번: 2021-26710